

Fate and Transport of Per- and Polyfluoroalkyl Substances in the Unsaturated Zone

Author:

Naod Negash

Guided research under supervision of:

Prof. dr. Jack Schijven

Drs. Arjen Wintersen

Abstract

In recent years, the group of compounds called PFAS (per- and polyfluoroalkyl substances) have been getting an increasing amount of attention. Most notable of the PFAS are PFOA and PFOS, due to their truly ubiquitous nature. In the Netherlands PFOA and PFOS are found virtually everywhere in the topsoil. Combined with the adverse health effects associated with exposure to these compounds, norms (i.e. criteria) for application of soil/sediment containing PFAS have recently been determined. However, questions are still present regarding the fate of PFAS in the unsaturated zone, and how the underlying groundwater will be affected. Thus, in this paper the fate and transport of PFAS in the unsaturated zone was investigated. The main processes affecting PFAS, and predominantly PFOA and PFOS, were delineated, quantified when possible, and described in a mathematical equation which describes reactive transport of PFOA and PFOS in the unsaturated zone. Furthermore, scenario characterization is discussed in the context of protecting groundwater in the Netherlands from PFAS leaching from the soil, and thus the concept of the "average Dutch situation" is also prevalent. Finally, a sensitivity analysis was carried out to determine the sensitivity of the retardation factor to certain parameters. The results showed that the solid-phase partitioning coefficient caused the largest changes in retardation by virtue of having the largest range of values. Steps for subsequent modelling work are suggested.

Definitions & Nomenclature	3
1. Introduction	5
1.1. Objectives	7
2. Processes Governing Fate and Transport	7
2.1. Advection, Dispersion & Diffusion	8
2.2. Solid-Phase Adsorption	9
2.2.1. Chain Length	11
2.2.2. Soil Composition	13
2.2.3. Solution Chemistry	15
2.2.4. Sorption Isotherms and Kinetics	17
2.2.5. Field vs. Lab Derived Partition Coefficients	18
2.2.6. Section Summary + Take-Home Message	19
2.3. Air-Water Interfacial Adsorption	22
2.3.1. Degree of Saturation	23
2.3.2. Sufactant Concentration	26
2.3.3. Molar Volume	29
2.3.4. Section Summary + Take-Home Message	31
2.4. (Bio)degradation	32
2.5. Conclusions	32
3. Mathematical Framework	34
4. Scenario Characterization	35
4.1. Hydrology of the System	36
4.2. Chemistry of the System	37
5. Modelling Exercise	39
5.1. Approach	39
5.2. Methods	40
5.2.1. Validation Case	40
5.2.2. Sensitivity Analysis	41
5.3. Results	43
5.3.1. Validation Case	43
5.3.2. Sensitivity Analysis	44
5.4. Discussion + Conclusions	47

6. Summary + Final Remarks.....	48
References	50
Appendix I : Modified HYDRUS-1D Model	54

Definitions & Nomenclature

ADE – the advection-dispersion equation. This equation describes the transport of a compound through a porous medium.

Attenuation – reduction of the concentration of a compound during transport.

“Average Dutch situation” - the “average Dutch situation” entails that a situation/scenario is representative for the Netherlands in a general sense. As such, if this scenario is modelled then the results would be representative for the Netherlands.

BTC – breakthrough curve. Is a curve that shows the change in concentration of a compound over time at a point downstream of a source. For a pulse injection (i.e. fixed-mass injection) of a compound that does not react or adsorb, the BTC takes the form of a bell-shape. For a continuous injection of the same compound, the concentration starts at the background concentration and increases to the maximum concentration, which is the concentration at the source (if there is no dilution).

Hazardous substance – substances/compounds whose input into groundwater should be prevented.

Non-hazardous substance – substances/compounds whose input into groundwater should be limited.

Input – any entry of a substance into the groundwater, either accidental or intentional, that causes pollution of the groundwater. This entry can be from either point or diffuse sources, and can be direct or indirect. Direct input is when the source of the substance/pollutant is at least partially and/or occasionally in direct contact with the groundwater table, indirect input is when the source is always located above the groundwater table.

NRT – a non-reactive tracer. In the context of this report it more specifically implies a non-adsorbing solute.

PFAS(s) – per- and polyfluoroalkyl substance(s); a large group of substances containing an alkyl chain with at least one hydrogen atom substituted with a fluorine atom.

PFAA(s) – perfluoroalkyl acid(s); a subgroup of PFASs. Consists of alkanes which are completely fluorinated (i.e. hydrogen atoms replaced by fluorine atoms), with an acidic headgroup.

PFCA(s) – perfluoroalkyl carboxylic acid(s) (e.g. PFOA)

PFSA(s) – perfluoroalkyl sulfonic acid(s) (e.g. PFOS)

Points of compliance (POCs) – are points in the groundwater system that are either physical or theoretical (i.e. based on model calculations). At these points, the concentration of a substance should be below a certain compliance value (i.e. norm), to ensure protection of the groundwater *locally* from pollution.

Receptor – any entity that can be adversely affected by a given pollutant. Examples are human health, (micro)organisms, the ecosystem, and groundwater.

Retardation factor – a factor that arises from the ADE of an adsorbing solute, with adsorption being described as an equilibrium process (i.e. instantaneous). The retardation factor is a measure for how much slower an adsorbing solute travels in a given system when compared to an NRT.

Surfactant – a compound that is amphiphilic: has a hydrophilic headgroup and a hydrophobic or lipophilic tail. As a result, surfactants often prefer to 'sit' on interfaces between two fluid phases (e.g. water-air, water-oil).

Worst-case scenario – in the context of leaching of contaminants in soil to the groundwater, a *worst-case scenario* would entail taking considerations that would expect to maximize the mobility of the contaminant. In such a case, the pollution of the groundwater is more likely, and in that sense is a *worst-case scenario*. The absolute worst-case scenario would be a transport of a compound which only goes advection (no dispersion or other attenuation processes). This is of course unrealistic, yet it would give the highest possible concentration in the groundwater.

1. Introduction

(1) In recent years, per- and polyfluoroalkyl substances (PFASs), and especially perfluorooctanoic acid (PFOA) and perfluorooctane sulfonic acid (PFOS), have been getting an increasing amount of attention in both the public and the scientific community (e.g. Ruffalo, Vachon, & Koffler, 2019). This is partly due to their ubiquitous nature, with PFAS having even been found as far as the Arctic (e.g. Young et al., 2007; Ahrens et al., 2011a; Xie et al., 2015), despite not having any significant sources nearby. This ubiquity is enforced by the persistence of some PFASs, meaning that they do not readily degrade or metabolize and thus tend to accumulate in biomass (Ding & Peijnenburg, 2013). The fact that they exhibit various physiochemical properties and are used in a variety of different industries and products, and thus enter the environment in several ways, also adds to their pervasiveness. Coupled with the toxic effects some PFASs have on humans and biota leads to concerns regarding their fate, and the consequences for humans and ecosystems.

(2) In the Netherlands, concerns regarding the possible adverse health effects of PFASs have ramifications on a variety of industries, one of which is the (re-)use and application of soil and sediment for building projects. In the Netherlands, chemical compounds which have been deemed as potentially dangerous to human and/or ecosystem health must conform to certain criteria (i.e. concentrations) to be eligible for application at a different site, for instance during building projects. In other words, if the concentration of one of these pollutants in a given batch of soil or sediment is above the norm, then this soil or sediment is not allowed to be applied. These criteria vary per compound and per classification of function of the ground use (i.e. what activities and practices will occur on the ground once construction is complete). In 2019, the RIVM published the current (temporary) criteria for application of soil or sediment containing PFAS (specifically PFOA, PFOS, and GenX; Wintersen & Otte, 2019). However, the memo indicates that it is uncertain whether these criteria sufficiently protect the groundwater or not, or even whether the current condition of PFAS contamination in Dutch soils is low enough to provide protection for the underlying groundwater. This has implications with regards to the goals of the European Commission (EC) and its member states, as per article 6 of the European Groundwater Directive (EGD; EC, 2006).

(3) In the EGD (EC, 2006), policy was created to protect groundwater quality from pollution. Article 6 of the EGD stipulates that input of pollutants to the groundwater should be prevented or limited, with input being defined as “any entry of a substance into groundwater from an activity, whether accidental or deliberate, point source or a diffuse source, that causes a release of a pollutant into groundwater”. Input can be direct or indirect: indirect input is when the contamination source is located outside the groundwater body (i.e. in or above the vadose zone), and direct input is when the source is located partially or completely within the groundwater body (see fig. 1). Whether inputs to the groundwater should be prevented or limited depends on the classification of the pollutant: for hazardous substances input should be prevented and for non-hazardous substances input should be limited such that no “deterioration or significant and sustained upward trends in the concentrations of pollutants in groundwater” is observed. While it is not clear whether PFOA and PFOS are considered hazardous

substances or not as per the EGD, considering they are deemed as Substances of Very High Concern (SVHC) in the Netherlands it would be prudent to learn more about their fate and transport in the unsaturated zone in order to protect the groundwater.

(4) In the Dutch report NOBO (VROM, 2007), the basis for the determination of criteria of pollutant concentration in soil/sediment with respect to the application of the soil/sediment (i.e. whether or not a given mass of soil/sediment is permitted to be applied at a site for a given function) is outlined. However, the determination of these criteria is primarily focussed on protection of receptors subject to exposure to the (contaminated) soil directly or indirectly through the food chain, and does not specify methods to consider transport of contaminants to the underlying groundwater. A receptor can broadly be defined as any entity that can be adversely affected by a given pollutant. In NOBO, these entities are human health, (micro)organisms in the ecosystem of interest as a proxy for ecosystem functioning, and agricultural produce. Protection of groundwater quality is also mentioned in NOBO but is not elaborated on. Thus, current compliance values for application of soil/sediment with respect to the varying soil functions (i.e. agricultural/natural, inhabited, and industrial) do not necessarily protect the groundwater sufficiently as per article 6 of the EGD. Considering this, an evaluation of PFAS transport from (surface) applied soil/sediment to the groundwater is imperative.

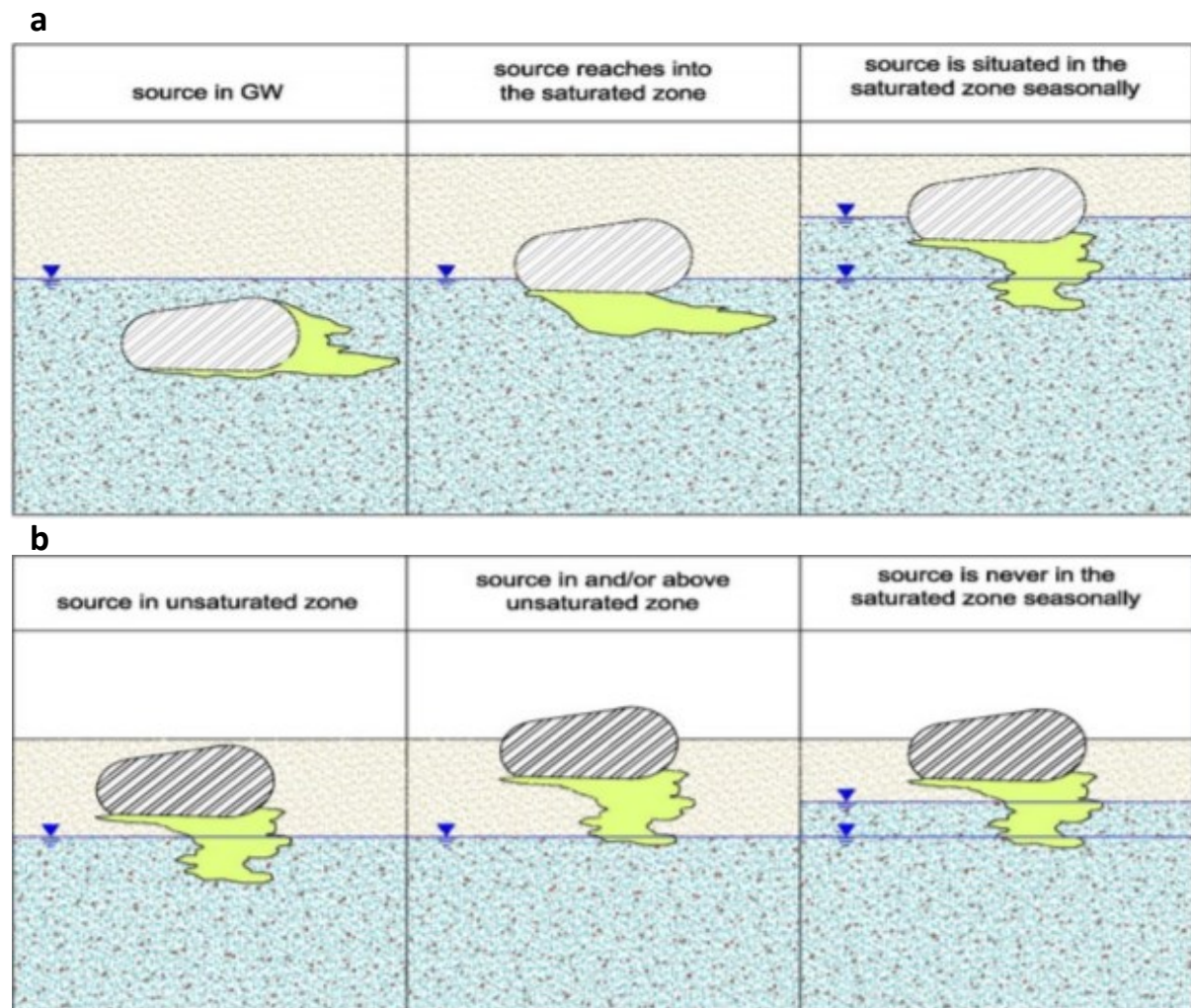


Figure 1 Illustration of what is meant by direct (a) and indirect (b) input of a pollutant into the groundwater. Grey stripes indicate source zone, green shaded area is the contaminant plume, and the blue arrow denotes the groundwater table. Image from guidance document on preventing and limiting direct and indirect inputs (EC, 2007).

(5) To assess the soil criteria for PFOA and PFOS in terms of the impact on groundwater, modelling tools can be employed which can simulate reactive transport and thus predict concentrations at the water table. The focus of this report is thus on how to model the transport of PFAS in the context of indirect input from surface applied soil/sediment, as opposed to determining the limit and compliance values themselves. This entails attaining a thorough understanding of the various processes affecting fate and transport of PFAS (especially PFOS and PFOA) in the unsaturated zone from the literature.

1.1. Objectives

(6) Following this, the objective of the report is twofold. First is to get a better understanding of the different processes affecting transport of PFASs (predominantly PFOS and PFOA) in the unsaturated zone: what are the processes and what are influences on them based on the literature. Where possible, a quantitative description of the processes and the influences on them will be given. Special attention is paid towards PFOA and PFOS because these two PFAS are the most frequently encountered in natural sediments, having been found in 89% of the tested locations in Wintersen et al. (2020a). Second is to get a description on how to model transport of surfactant PFAS, along with the results and insights of an initial modelling effort. However, the overarching goal of the report is to serve as a source of information and ideas for future modelling efforts directed towards modelling transport of (surfactant) PFASs in the unsaturated zone. This especially in the context of evaluating or determining suitable criteria in surface-applied soil/sediment in the Netherlands. As such, the concept of the “average Dutch situation” is important since many of these processes affecting transport are both spatially (i.e. geographically) and temporally variable. This concept will be discussed further in chapter 4.

2. Processes Governing Fate and Transport

(7) This chapter will focus on the various processes that govern fate and transport of PFAS in the context of PFAS transport from surface applied soil/sediment to the groundwater: discussion will be on the effect these processes have on transport, and the factors that influence these processes. Special attention will be given to surfactant PFAS like PFOS and PFOA. These processes include transport processes like advection, dispersion, and diffusion. Other relevant processes are adsorption to the solid-phase and fluid-fluid interfaces. This latter process is not relevant for all PFAS, but is important for PFOA and PFOS (e.g. Lyu et al., 2018; Brusseau et al., 2019). While these two compounds do not appear to degrade (de Voogt, 2010), precursor PFAS to PFOA and PFOS do exist and so (bio)degradation will also be discussed. Volatilisation will not be discussed since neither PFOA nor PFOS are volatile compounds (OECD, 2002; EPA, 2002; Ding & Peinenburg, 2013), and so are not expected to exist in the gas phase in the soil atmosphere. Other processes that will not be considered are surface runoff and wind-erosion. Below is a conceptualization of the relevant processes for the scenario of surface applied soil/sediment (fig. 2). The ones that will be discussed in this chapter are **C** (advection/dispersion/diffusion), **D** (solid-phase adsorption), **E** (air-water interfacial adsorption), and **F** (degradation).

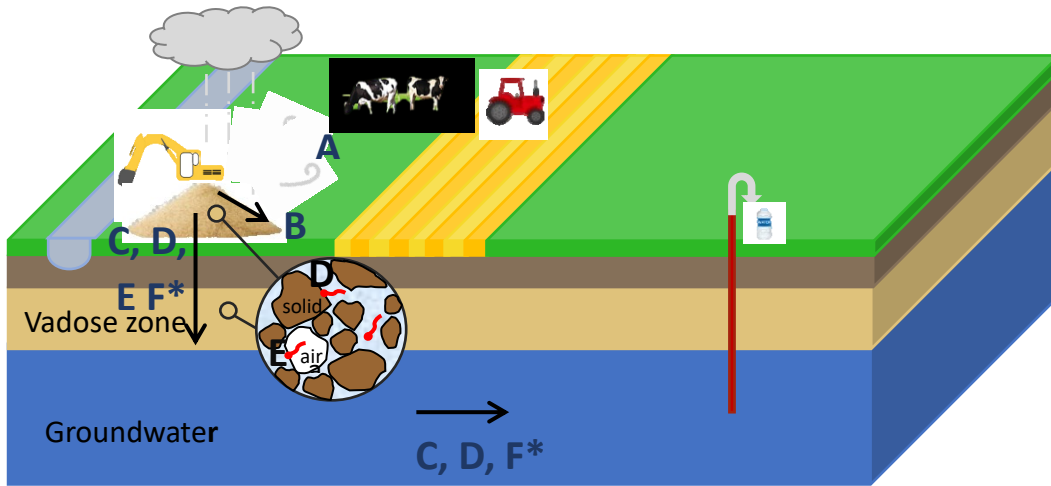


Figure 2 Conceptual model of a scenario in which sediment is excavated from a canal and deposited on the banks. The depicted processes are: (A) wind erosion, (B) runoff, (C) advection/dispersion/diffusion, (D) solid-phase adsorption, (E) air-water interface adsorption, and (F) degradation of precursors. *It is not clear whether degradation of precursors will occur under conditions expected in these environments.

2.1. Advection, Dispersion & Diffusion

(8) One group of processes which are inherent to transport of all solutes in porous media, for both saturated and unsaturated conditions, are transport processes. Individually, they are advection, dispersion, and diffusion. However, before each of these processes are discussed, a distinction needs to be made between flow and transport. The term ‘flow’ is used to describe the flow of a medium (e.g. water) in another medium (e.g. porous sand), as opposed to ‘transport’, which describes the transport of a compound in the flowing medium. Intuitively, it is clear to see that the two are linked, since the transport of a solute is very much dependent on the flow conditions. Similarly, in the case of water flow in the unsaturated zone, the flow is dependent on hydrological conditions (e.g. precipitation, water-table depth) and properties of the sand (i.e. soil hydraulic properties). To better understand the relationship between flow and transport, one can examine the commonly used (e.g. PEARL, SWAP, HYDRUS, PHREEQC) 1D advection-dispersion equation (ADE), which describes (vertical) transport, in its simplest form:

$$\frac{\partial(\theta \cdot C)}{\partial t} = -\frac{\partial(\theta \cdot v \cdot C)}{\partial z} + \frac{\partial}{\partial z} \left(\theta \cdot D \cdot \frac{\partial C}{\partial z} \right) \quad (1)$$

(9) Where θ is the water-content [$L^3 \cdot L^{-3}$; volume liquid/total volume], C is the concentration in solution [$M \cdot L^{-3}$; mass of compound in solution/volume liquid], t is time [T], v is the velocity [$L \cdot T^{-1}$], z is the depth [L], and D is the hydrodynamic dispersion coefficient [$L^2 \cdot T^{-1}$]. The dispersion coefficient, which represents both dispersion and diffusion, is given by:

$$D = \alpha_L \cdot v + D_e \quad (2)$$

(10) where α_L is the dispersivity [L] and D_e is the molecular diffusion coefficient [$L^2 \cdot T^{-1}$]. α_L is a property of the porous medium while D_e is a property of a compound in a given medium.

(11) Equation 1 effectively describes the transport of a non-reactive (and non-adsorptive) solute, since only transport terms are present. From this equation, and eq. 2, the effect of flow can be seen in two variables/parameters: v and D . The velocity, v , is directly influenced by flow as it is the velocity of the flow. The dispersion coefficient, D , is comprised of two terms to represent two processes: dispersion, which is a macroscopic phenomenon and is a result of the tortuous flow-paths in porous media, and molecular diffusion, which is a microscopic phenomenon and is a result of Brownian motion of

particles. The effect of flow on D can be seen in the dispersion component: for higher velocities there is increased dispersion (see eq. 2). Since dispersion (and diffusion) serve to attenuate transport (i.e. reduce the peak concentration of a breakthrough curve of a pulse injection as a result of mixing with resident water), velocity also attenuates transport. This highlights that the velocity field has an important role in describing the fate and transport of a solute in a porous medium, and since the velocity field is a description of the flow conditions it means that the flow strongly influences transport.

(12) Since flow has an integral part in describing transport, it is perhaps prudent to briefly discuss flow in the context of the unsaturated zone. In the unsaturated zone, water infiltrates from the surface (i.e. top of a soil profile) because of excess precipitation, and percolates down to the groundwater table. The amount of water that infiltrates in a given time period is equal to the amount of precipitation minus the evapotranspiration and runoff in the same period. In the case of steady-state infiltration (i.e. constant infiltration rate over time), with the groundwater table at a certain depth, a steady-state water-content profile will be established which is not homogeneous (i.e. the water-content will vary in depth). The infiltration rate is essentially a flux of water, and due to conservation of mass the flux of water must be the same at every point in the soil profile. However, since the water-content is not constant in depth, and since $v = q/\theta$ (where q is the infiltration rate), the velocity will also vary in depth (i.e. the velocity field is not homogeneous). The resulting (1D) velocity field and water-content profile, which is what is necessary to model (1D) transport, is dependent on several things: 1) infiltration rate, 2) depth of the groundwater table, and 3) soil-hydraulic properties (e.g. soil-water retention curve & hydraulic conductivity). Another way to see this is that the velocity field water-content profile are dependent on the boundary conditions (i.e. infiltration rate and groundwater table depth), and system properties/parameters (i.e. soil-hydraulic properties). In reality, the infiltration rate and depth of groundwater table vary in both space (i.e. from location to location) and time. Similarly, the soil-hydraulic properties also vary from location to location. Thus, 1D velocity fields vary in time at any given location, and also in space at any given time.

(13) To summarize, the most important points of this section are:

- In the context of groundwater (i.e. both unsaturated and saturated zones), flow describes the movement of water in the porous medium (i.e. soil), and transport describes the movement of compounds in the water.
- Transport of solutes in porous media is described by some variation of the ADE (eq. 1). If the solute undergoes adsorption or other non-equilibrium reactions, then they need to be reflected in the equation.
- Transport of solutes is very much dependent on the flow conditions (i.e. the velocity field and water-content profile).
- Dispersion and diffusion (and thus also velocity; see eq. 2) attenuate transport of solutes due to mixing with resident water.
- Flow conditions, and more specifically the vertical 1D velocity field and water-content profile, are dependent on infiltration rate, groundwater table depth, and the soil-hydraulic properties.
- In a given area/region (e.g. the whole of the Netherlands), the vertical velocity field and water-content profile in the unsaturated zone will vary in both space and time.

2.2. *Solid-Phase Adsorption*

(14) The term adsorption, and particularly in reference to solid-phase adsorption, is used to describe several mechanisms/interactions that bind a compound to the surface of a solid. There are several types of bonds between a compound and a solid surface (see fig. 3), and they can vary in strength.

Figure 3 (Li et al., 2018) shows *possible* adsorption mechanisms for PFCAs and PFSA, and suggests that both electrostatic and hydrophobic interactions could play an important role. To be clear, it has not been established that these mechanisms occur indefinitely, but rather are hypothetical based on interpretation of experimental data. Each of these individual mechanisms can be defined by equations to account for their effects. This would be what is called a ‘speciation model’ (e.g. Spijker et al., 2009; Verschoor et al., 2006), and requires detailed information of both the system and the nature of these bonds and mechanisms (i.e. number of binding sites & thermodynamics of the different reactions). Although the literature was not searched thoroughly for information required to set up a speciation model, a brief search determined that the information is not readily available, if at all.

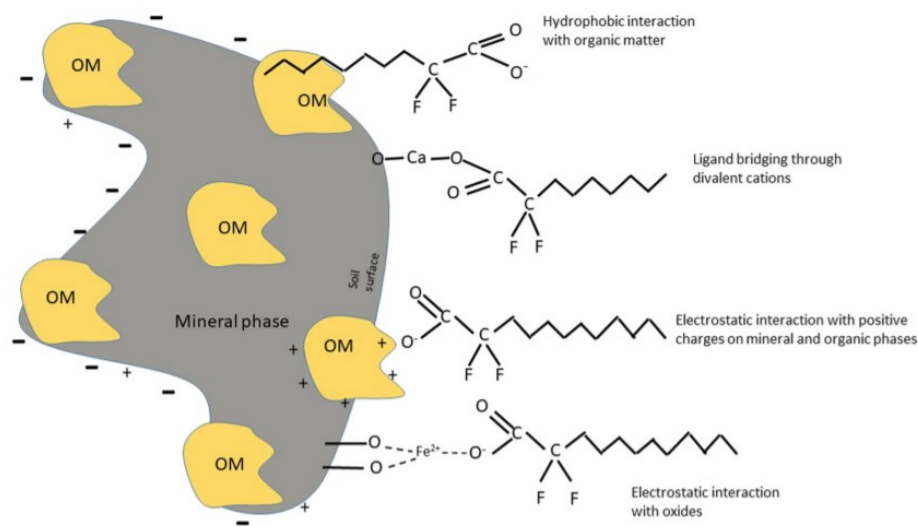


Figure 3 Conceptualization of possible adsorption mechanisms relevant for PFCAs and PFSA. Image from Li et al., 2018.

(15) Another way to describe adsorption is to use a partitioning coefficient (e.g. K_d or K_{oc} ; Verschoor et al., 2006), which essentially lumps all of these mechanisms together into one parameter (EPA, 1999; Schwarzenbach et al., 2003). Due to time constraints, only one of these avenues was investigated, and due to the large body of literature regarding the partitioning behaviour it seems like the better option. The solid-phase partitioning coefficient, K_d , is defined as:

$$K_d = \frac{C_s(eq)}{C_{aq}(eq)} \quad (3)$$

(16) Where K_d is the partitioning coefficient [$L^3 M^{-1}$; volume liquid/mass solid], $C_s(eq)$ is the equilibrium concentration of the adsorbing compound on the solid [$M M^{-1}$; mass of compound adsorbed on solid/mass solid], and $C_{aq}(eq)$ is the equilibrium concentration in solution [$M L^{-3}$; mass of compound in solution/volume liquid]. Another commonly reported partitioning coefficient for organic compounds is the organic-carbon (OC) normalized K_d :

$$K_{oc} = \frac{K_d}{f_{oc}} \quad (4)$$

(17) Where K_{oc} is the OC normalized partitioning coefficient [$L^3 M^{-1}$; volume liquid/mass OC], and f_{oc} is the OC fraction [$M M^{-1}$; mass OC/mass solid]. The implication of using a K_{oc} is that it implies adsorption to OC is the dominant mechanism, and thus normalizing K_d to f_{oc} would reduce variability in K_d between soil samples.

(18) The lumping of all the mechanisms simplifies describing the adsorption process, since only a single parameter is necessary. However, it also makes it difficult to describe the adsorption process for a given soil/sediment *a priori*, since the effect of conditions (e.g. pH, organic-carbon fraction) is not explicitly defined. While K_{oc} , which is determinable from other sources, already makes it easier to say something about the solid-phase adsorption *a priori* if f_{oc} is known, significant variation can sometimes be seen in K_{oc} for the same compound (e.g. see table 5). This limits its predictive capability. Nevertheless, due to the lack of information regarding the individual mechanisms of PFAS adsorption, and the comparatively much larger body of information regarding partitioning coefficients, the latter description of the adsorption process is discussed here. For the case of PFAS, with emphasis on PFOA and PFOS, several factors that influence the partitioning behaviour have been studied in the literature. The ones that will be discussed in further detail below are chain length of the alkyl chain, soil composition (i.e. organic carbon content & clay-content), solution chemistry (i.e. pH & ionic strength), sorption isotherms and kinetics, and field vs. lab determined partitioning coefficients. This last aspect is not so much a factor that influences the adsorption process but is something to consider when obtaining partitioning coefficients from the literature for use in modelling simulations.

2.2.1. Chain Length

(19) Several studies have reported a positive correlation between chain length and partitioning coefficient, either K_d or K_{oc} (e.g. Higgins & Luthy, 2006; Enevoldsen & Juhler, 2010; Kwadijk et al., 2010; Chen et al., 2015). In all these studies, adsorption increases with each $-CF_2$ moiety, although the exact relationship (i.e. the slope of the regression) varies per study. Table 1 below summarizes the slope of the regressions for PFCAs and PFSA, with the slope indicating change in log units of either K_d or K_{oc} for each added $-CF_2$ moiety. Higgins & Luthy (2006) conducted sorption experiments on 5 different natural sediments of riverine and lacustrine origin, and with varying characteristics. Although the regression is not shown in the paper, it is assumed a linear regression was used to determine the relationship between chain-length and $\log(K_d)$. They found that with each added moiety the partitioning coefficient would increase by around 0.5-0.6 log units for both PFCAs (4 considered; C7-C10. **Note:** carbon in COOH group is not included) and PFSA (2 considered; C8 & C10). It is not clear whether the distribution coefficient they refer to is K_d or the K_{oc} , but it is assumed they are referring to the former. When the data was analysed independently, K_{oc} vs. chain length regressions showed an increase of 0.41-0.45 and 0.48-0.49 log units for each additional moiety for PFCAs and PFSA, respectively, albeit the number of compounds considered was small. It should also be noted that the number of sediments analysed to determine the K_{oc} is also quite small (maximum is 5, and only 2 for PFOA).

(20) The dependencies of K_{oc} on alkyl chain length agree quite well with regressions done by Chen et al. (2015), who found that $\log K_{oc}$ increased for each additional moiety by 0.49 and 0.41 log units for PFCAs (7 considered) and PFSA (3 considered), respectively, with $R^2 \geq 0.969$ for both regressions. The samples used in this study were taken from different sites at two locations in China, Lake Taihu ($n=22$) and the Liao River ($n=25$). They looked at partitioning in both the sediment on the bed and the suspended particulate matter (SPM), yet only the sediment-derived $\log K_{oc}$ was used in the chain length vs. $\log K_{oc}$ regression. Also, the partitioning coefficients were field-based, meaning that the concentrations in the respective compartments (i.e. sediment and overlying water) were used to derive the partitioning coefficients. This contrasts with the coefficients from Higgins and Luthy (2006) since they were derived from batch experiments. Interestingly, when the $\log K_{oc}$ values are compared to those of Higgins & Luthy the values in Chen et al. are consistently higher for any given PFAS, even though similar regressions were found for $\log K_{oc}$ and chain length. The discrepancy in $\log K_{oc}$ values was also seen in a review by Zareitalabad et al. (2013) who found that K_{oc} values determined from the

field were consistently higher than values measured in the lab, yet this will be discussed in more detail in section 2.2.5..

(21) Kwadijk et al. (2010) also looked at the relationship between $\log K_{oc}$ and carbon chain length from samples throughout the Netherlands and found that each moiety contributed 0.4983 log units for PFCAs (3 considered; C7-C9) and 0.2613 log units for PFSA (2 considered; C4 and C8). Enevoldsen & Juhler (2010) analysed sorption of select PFAS on two types of soil; one characterised as sandy (94% dw) and the other as clayey (37% dw). Instead of chain length, they compared the $\log K_{oc}$ with the molecular weight and found a good linear fit ($R^2 = 0.9928$) for the sandy soil. However, the same was not found for the clay soil, where a quadratic fit explained the relationship well ($R^2=0.9956$). It is unclear whether they separated the PFAS into different classes, but it appears as though the regression was made for all the PFAS they analysed (both PFCAs and PFSA).

(22) Table 1 below summarizes the slope of the regressions for PFCAs and PFSA, with the slope indicating change in log units of either K_d or K_{oc} for each added $-CF_2$ moiety. This data could potentially be used to describe the partitioning of PFCAs and PFSA that otherwise do not have much data on their partitioning behaviour. For example, if the K_d or K_{oc} is known for PFOA, but not for PFBA (C3), then the regression of Pereira et al. (2018) could be used. This is not ideal, since actual data on sorption behaviour of PFBA would be preferred, but should that information be lacking then this is a viable option.

Table 1 Summary of the slopes of the linear regressions between either $\log(K_d)$ or $\log(K_{oc})$ and carbon-chain length of the alkyl chain of PFCAs and PFSA, as reported in the various studies. The slope thus indicates the number of log units K_d (or K_{oc}) would increase per added $-CF_2$ moiety: the K_d increases because the slope is positive. *This study made a regression between $\log(K_{oc})$ and molecular weight as opposed to chain length, and included all PFAS tested (some PFCAs and PFSA).

Source	PFCAs		PFSA		Comments
	Log(K_d)	Log(K_{oc})	Log(K_d)	Log(K_{oc})	
Higgins & Luthy (2006)	0.5-0.6	0.41-0.45	0.5-0.6	0.48-0.49	4 PFCAs (C7-C10) and 2 PFSA (C8 & C10) considered. For regressions with K_{oc} , $R^2 \geq 0.986$
Chen et al. (2015)	-	0.49	-	0.41	7 PFCAs (C5-C11) and 3 PFSA (C4, C6, & C8) considered. For both regressions $R^2 \geq 0.969$.
Kwadijk et al. (2010)	-	0.4983	-	0.2613	3 PFCAs (C7-C9) and 2 PFSA (C4 & C8) considered. For regression for PFCAs R^2
Ahrens et al. (2010)	-	0.52-0.75	-	0.51	5 PFCAs (C6-C10) and 2 PFSA (C6 & C8) considered. No regression shown.
Pereira et al. (2018)	-	0.60	-	0.83	8 PFCAs (C3-C10) and 3 PFSA (C4, C6, & C8) considered. No R^2 shown.
Enevoldsen & Juhler (2010)*	-	0.0275*	-	0.0275*	Slope was for all PFAS tested, which consisted of some PFCAs and PFSA, and is for the sandy soil. $R^2 = 9928$
Guelfo & Higgins (2013)	0.45-0.51	-	-	-	3 sediments analysed; for 2 of them 6 PFCAs considered (C5-C10), and C7-C9 for other sediment.

2.2.2. Soil Composition

Organic Carbon Content

(23) The main point of contention when it comes to characterizing the adsorption behaviour of PFASs based on single parameters is whether organic carbon is the key factor controlling sorption. If so, then the use of K_{oc} is justified. While the K_{oc} is useful in describing the sorption behaviour of non-ionic organic contaminants (Schwarzenbach et al., 2003), due to the anionic head of perfluoroalkyl acids (PFAAs; like PFCAs and PFSAAs) the K_{oc} might not be sufficient to accurately describe the sorption process since electrostatic interactions may have a pronounced role. While some studies have found strong correlations between K_d and OC (e.g. Higgins & Luthy, 2006; Miao et al. 2017; Milinovic et al., 2015; You et al., 2010), others found no or weak correlations (e.g. Becker et al, 2008; You & Pan, 2010). Furthermore, some studies that did show a good relationship were conducted at a fixed pH and so the relationship does not necessarily describe all systems. Li et al. (2018) did a rigorous review on factors influencing PFAS sorption by collating data from 28 peer-reviewed studies, and only considered natural sediments. Data on all their regressions can be found in the Supplementary Information of the study. Their analysis on the effect of OC on K_d for a range of PFAS generally found weak correlations. Of the PFASs with datasets greater than 10 they found significant relationships ($P < 0.05$) for PFOS ($n=178$), PFOA ($n=147$), PFNA ($n=87$), PFDA ($n=57$), PFHpA ($n=54$), PFHxA ($n=50$) and FOSA ($n=50$). However, all of these relationships had an $R^2 \leq 0.35$, except FOSA which had an R^2 of 0.70. Nevertheless, the regression of PFNA was heavily skewed by a few very high OC values, and when they were removed the regression was no longer significant. Some other PFAS were significantly correlated but their sample size was small (≤ 8), and some of these were also levered by a high OC value and didn't have significant relationships once these values weren't considered. So if the entire dataset is considered it is apparent that simply using the K_{oc} is not suitable to describe the sorption behaviour of PFAS in all environments. As a visual reference, figure 5 shows the spread of K_d vs. OC for PFOS, indicating that using a single K_{oc} value would have substantial uncertainty in its predictive capability. Unfortunately, the raw data for this plot, and the rest of the data in Li et al. (2018), is not readily available.

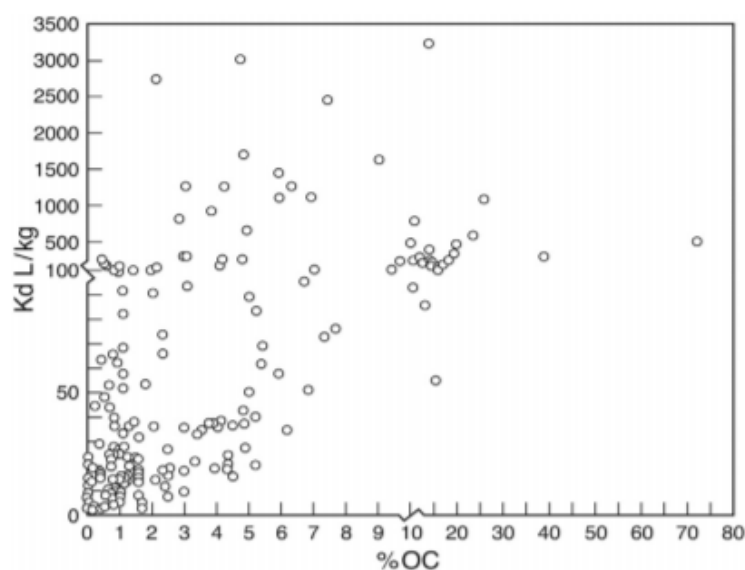


Figure 4 K_d plotted against the %OC for PFOS. Image from Li et al. (2018).

(24) To further illustrate this, a comparison of the results from Higgins and Luthy (2006) and Johnson et al. (2007) was made (Table 2). These two studies also measured the specific surface area (SSA) of the sediments, making it ideal for comparison. When the K_d was normalised by the SSA, the highest partition coefficient was for sediment 1 (Ottawa sand) from Johnson et al., despite having no detectable organic carbon. When compared to sediment 5 of Higgins and Luthy the value is two orders of magnitude greater even though sediment 5 consists of ~10% organic carbon. Similarly, sediment 4 (goethite) from Johnson et al. also had no organic carbon, yet the normalised K_d was twice as high as the value for sediment 2 from Higgins and Luthy. The difference is even more pronounced for the non-normalized K_d . This highlights that there are other factors that could have a significant impact on PFAS sorption, such as electrostatic interactions.

(25) The main conclusion from this is that the conventional way of describing the partitioning behaviour of organic pollutants, namely with K_{oc} , does not appear to be valid for PFOA and PFOS. The fact that significant relationships between these two compounds and OC was found indicates that OC does in fact have an influence, but the lack of good fit suggests that the effect of other factors cannot be neglected.

Table 2 Comparison of sorption data of PFOS from two sources. All sediments used in Higgins & Luthy (2006) are of natural origin, but only sediments 1,3, and 5 from Johnson et al. can be considered natural; sediments 3 and 5 were pure mineral phases. **Note:** the sediment samples differ between the two studies. The two yellow rows and the two green rows signify the sediments they are compared to in paragraph 25 (i.e. yellow compared to yellow & green compared to green).

Higgins & Luthy (2006):					Johnson et al. (2007)				
PFOS					PFOS				
Sediment	BET Surface Area [m ² /g]	K _d [L/kg]	K _d /SSA [L/m ²]	f _{oc} [-]	Sediment	BET Surface Area [m ² /g]	K _d [L/kg]	K _d /SSA [L/m ²]	f _{oc} [-]
1	18	17.1	0.953	0.0248	1	0.002	2.81	1405	0
2	27	1.82	0.067	0.0102	2	10	5.31	0.531	0.02
3	27	14.2	0.527	0.0434	3	-	7.52	-	0.025
4	89	-	-	0.0056	4	58	7.88	0.135	0
5	8	45.8	5.72	0.0966	5	6	8.9	1.483	-

Clay content, CEC, and AEC

(26) It has been established that electrostatic interactions can play an important role in PFAS adsorption, and as such (clay) minerals need to be considered since their surfaces often carry charge. Clay minerals can have both positively and negatively charged surfaces, both of which have an influence on adsorption of anionic PFASs. The surface charge of adsorbents is related to the pH (Ferrety et al., 2012): as pH increases the net surface charge becomes more negative due to deprotonation of surface functional groups (Du et al., 2014). While the clay-content itself is not a measure of the surface charge, it can be considered as a measure of the potential number of binding sites (along with OC). More accurate measures of the potential number of binding sites are the CEC and AEC, and considering the negatively charged head of anionic PFAAs the AEC would intuitively be more important. However, CEC can also be important if there are enough divalent cations present to facilitate divalent cation bridging (Du et al. 2014; see also fig. 3).

(27) Li et al. (2018) also investigated the statistical relationships between these three sorbent properties (i.e. clay content, CEC, & AEC) and K_d . Only four of the studies they looked at included the clay content of the sediments (n = 32), and only four compounds had more than 10 data points: PFBS, PFOS, PFOA, and PFDA. None of them had a significant relationship between K_d and % clay. Only for PFPeA a statistically significant relationship ($R^2=0.88$, n=6) was found, but the sample size was quite

small. It should be noted, however, that the definition of what is considered clay can vary internationally, and since it is not sure if the definition is consistent among these studies this could be a source for error. Even fewer studies reported CEC, and even less reported AEC, and so relationships are tentative. A significant relationship was found between K_d and CEC for PFBS ($R^2=0.73$, $n=6$), however, for PFOA ($n=18$) and PFOS ($n=10$) no significant relationship was found and CEC barely explained the sorption variability of PFOA ($R^2=0.07$). So from this it is clear that is insufficient to describe the sorption behaviour by any of these individual soil properties alone. Li et al. point out that often soil properties are dependent on each other and/or correlated. For example, soils with high %clay also generally have high $f_{oc,r}$, and as mentioned above CEC depends on pH and %clay, but also on organic matter content. For this reason, they say it is necessary to consider the role of multiple properties simultaneously to accurately describe the sorption behaviour.

(28) Aside from clay content, a high iron content can also be important since iron oxides and hydroxides on the surface of adsorbents can serve as positively charged sites for the negatively charged head of anionic PFAAs. In the microcosm experiments of Ferrey et al. (2012), relatively high adsorption coefficients were found in the beginning of the experiment and attributed to the sorption to positive surfaces associated with iron: either iron minerals such as goethite and magnetite, or Iron(II) or Iron (III) cations adsorbed to the surface of other minerals. Interestingly, when looking at sediment 4 (goethite) of Johnson et al. in table 2, the SSA normalized K_d is lower than for the Ottawa sand (sediment 1), despite that at the pH conditions of the experiment the silica charge densities are expected to be net negative while for the goethite it is expected to be net positive (Johnson et al., 2007). This further illustrates the fickle sorption behaviour of PFASs. Like with OC, none of the aforementioned factors alone can describe the partitioning behaviour of PFAS.

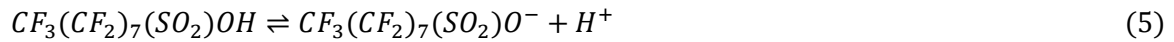
2.2.3. Solution Chemistry

pH

(29) As stated above, the pH of the solution influences the surface charge of adsorbents (both organic matter and mineral phases), and as such has an influence on electrostatic interactions. This is evidenced in Higgins and Luthy (2007), who found a linear decreasing trend between $\log(K_d)$ and pH. The slopes of the regressions were quite similar for 4 different PFASs, with each increasing unit in pH resulting in $-0.37 \log K_d$ units for all PFASs (PFOA, PFNA, PFDA, PFUnA, PFOS, and PFDS). However, at pH 7.5 both PFUnA and PFDS (the longest chained PFAAs considered) exhibited a sharp drop in $\log K_d$, and so were not considered in the regression. It was hypothesized that this was due to an increase in dissolved organic carbon (DOC) as a result of the increasing pH, and thus perhaps adsorption to DOC of longer chained PFAAs would result in an overestimation in their concentration in solution. However, analysis of DOC showed relatively constant concentrations suggesting this was not the cause for the drop. The slope of the regressions of Higgins & Luthy agree quite well with those of Pereira et al. (2018), who reported an average slope of -0.32 for a host of PFASs. Johnson et al. (2007) also looked at the relationship between the amount of PFAS sorbed to the goethite and kaolinite mineral sediments and pH and found a similar trend. They said, as did Higgins and Luthy, that this suggests that electrostatic interactions do play a role in PFAS sorption since increasing the pH makes the surface charge become more negative. At higher pH electrostatic repulsion increases since the PFAA's are anionic (i.e. headgroup have negative charge), resulting in a lower K_d . It should be noted, however, that the trend of decreasing K_d with increasing pH was not always observed. Some studies actually found the opposite trend (increased adsorption for increased pH; e.g. You et al., 2010) in the presence of divalent cations (Du et al., 2004), which was explained by increased negative charge on adsorbent surfaces and increased divalent cation bridging.

(30) When looking at the analysis done by Li et al. (2018), they found no statistically significant relationship between K_d and pH for PFOS ($R^2=0.06$, $n=27$, pH range 2.5-8.5) or for PFOA ($R^2=0.07$, $n=36$, pH range 4.5-10). Significant relationships were found for EtFOSAA ($R^2=0.57$), MeFOSSA ($R^2=0.67$), and PFDS ($R^2=0.65$), but these datasets were not as large ($n=10$).

(31) Aside from affecting the surface charge of sorbents, pH also affects PFAAs directly, namely whether the PFAA is in its acidic form or conjugate base. Since PFAAs like PFOS and PFOA are acids, they dissociate in solution at a certain pH. For PFOS the dissociation reaction looks like:



With the acid dissociation constant, K_a , being defined as:

$$K_a = \frac{[CF_3(CF_2)_7(SO_2)O^-] \cdot [H^+]}{[CF_3(CF_2)_7(SO_2)OH]} \quad \text{and} \quad pK_a = -\log(K_a) \quad (6)$$

(32) Where the brackets [] denote the concentration (i.e. $[H^+]$ is concentration of H^+ ions in solution). The pH at which an acid dissociates is determined by the pK_a : if $pH > pK_a$ then it will be in anionic form (i.e. conjugate base), if $pH < pK_a$ then it will be in neutral (i.e. acidic) form, and if $pH = pK_a$ then there will be equal concentrations of both forms. Since electrostatic interactions seem to be important in describing the adsorption behaviour of PFAAs, the form in which a PFAA is in could have ramifications for adsorption, although from the literature it is not entirely sure what these ramifications would be in a quantitative sense. However, the pK_a for PFSA is so low that they will always completely dissociate in the environment (Ding & Peijnenburg, 2013), and while the pK_a for PFCAs (especially PFOA) is still being debated, the highest pK_a reported is 3.8 (Burns et al., 2008). As such, PFOA is also expected to generally be in its ionic form in the environment. To get an idea of the difference in adsorption behaviour between anionic and neutral PFCAs (PFOA in particular), experiments done at sufficiently low pH would need to be compared with those done at higher pH's for similar sediments. However, then you would run into the problem of differentiating between the effect of changing pH on sorbent characteristics (i.e. surface charge) and form of PFOA. Considering this would be very difficult to accomplish, if not impossible, and the fact that PFOA is expected to mostly exist in its ionic form in natural environments, there is little added benefit to determine this. However, if conditions made it favourable for PFOA to protonate (i.e. sufficiently low pH), one added complication would be the marked increase in volatility (Ding & Peijnenburg, 2013; Vierke et al., 2013). Nevertheless, as stated previously, such conditions are not expected to occur in the environment.

(33) It is evident that pH will have an effect on adsorption due to its effect on the surface charge of solid surfaces and the fact that electrostatic interactions do play an important enough role in the adsorption behavior. However, like with the other influences no satisfactory regression could be made and thus the effect of pH on K_d (or K_{oc}) remains unquantified.

Ionic Strength & Solution Composition

(34) Other system properties that have been shown to influence adsorption of PFASs are the ionic strength and the solution composition, namely the presence of specific cations. Higgins & Luthy (2006) and Li et al. (2018) point out that it's difficult to analyse the influence of ionic strength (or pH) on sorption independently since changes in ionic strength also affect pH (and vice versa). However, when looking at the presence of cations, several studies have shown a positive correlation between cation concentration and K_d (e.g. Higgins & Luthy, 2006; You et al., 2010; Chen et al., 2012). Higgins and Luthy found a positive correlation between Ca^{2+} and K_d , with each log unit $[Ca^{2+}]$ contributing 0.36 log K_d units, but did not find any correlation between K_d and Na^+ . Instead of divalent cation bridging, they

proposed that the Ca^{2+} reduced the electrostatic effect of negatively charged functional groups, which would not be the case for Na^+ . You et al. (2010) investigated the effect on PFOS sorption of increased CaCl_2 at constant pH and found that at pH 7.0 sorption increased 3-fold when CaCl_2 concentration increased from 5 mM to 500 mM, and by a factor of 6 at a pH for the same concentration increase. This supports the bridging effect divalent cations have, but they say it can also be explained by the salting out effect or reduction in surface charge. The salting-out effect describes the reduced solubility of organic compounds in saline solutions. For example, the solubility of the salt PFOS-K drops from 370 mg L^{-1} in freshwater to 25 mg L^{-1} in filtered seawater (OECD, 2002). Pereira et al. (2018) did not make a regression, but also found that the presence of cations increased adsorption for PFCAs of intermediate chain-length (C5-C8) and PFHxS (C6 of PFSA). They looked at the effect of three different cations in solution (Al^{3+} , Ca^{2+} , and Na^+), and found that they increased adsorption in the following order: Al^{3+} (2 mM) > Ca^{2+} (5 mM) > Ca^{2+} (3 mM) = Na^+ (10 mM). Chen et al. (2012) investigated the effect of salinity (i.e. artificial seawater composition) and cations in solution. They found strong positive regressions between $\log(K_d)$ and the log of salinity (slope=+0.48) and $\log(\text{Mg}^{2+})$ (slope=+0.52) and $\log(\text{Ca}^{2+})$ (slope=+0.5). Having said this, however, from the analysis of Li et al. (2018) no significant relationship between K_d and Ca^{2+} was found for PFOS (n=32) or PFOA (n=7).

2.2.4. Sorption Isotherms and Kinetics

(35) Another vital aspect with regards to characterizing the adsorption behaviour is the sorption isotherm and kinetics. Du et al. (2014) looked at the adsorption kinetics and isotherms of different types of adsorbents (i.e. not natural sediments). They found a wide range in equilibration times (i.e. time for the adsorption process to reach equilibrium such that no change in concentration is observed), ranging from 1h to 168h, with no discernible difference between PFOS and PFOA for most of the adsorbents. More interesting, however, are the equilibration times for natural sediments. Miao et al. (2017) looked at sorption of PFOA on natural sediments (n=10) and found that equilibrium was generally achieved within 24h. Johnson et al. (2007) found similar equilibration times (22-24h) for PFOS for their sediments. You et al. (2010) and Pan et al. (2008) also equilibrated their samples for 24h (studying PFOS sorption), even though the kinetic experiments in the latter study showed apparent equilibrium after 8h. However, Higgins & Luthy (2006) found considerably longer equilibration times (between 190-240h).

(36) With respect to the isotherms, most studies used the Freundlich and/or linear isotherm (i.e. eq. 3) to describe the adsorption behaviour at different concentrations. The Freundlich isotherm is a common way to describe adsorption to heterogeneous media, and differs from the linear isotherm in that it is not linearly related to C_{aq} :

$$C_s = K_f \cdot C_{aq}^n \quad (7)$$

(37) Where K_f is the Freundlich coefficient [$\text{M M}^{-1} (\text{M L}^{-3})^{-n}$], and n is a constant at a particular temperature [-]. Note that like in eq. 3, C_s and C_{aq} in eq. 7 are the equilibrium concentrations. From this, an expression for K_d as function of aqueous concentration can be obtained:

$$K_d = K_f \cdot C_{aq}^{n-1} \quad (8)$$

(38) Li et al. (2018) say that sorption isotherms for ionizable solutes are dependent on pH and the saturating cation on the sorbent surface. In the experiments done by Higgins and Luthy (2006), the isotherms were described by the Freundlich isotherm (concentration ranges depend on the substance; see table 5 for more details). Miao et al. (2017) fitted both linear and Freundlich isotherms for PFOA and found that the former had a better fit. They also conducted desorption experiments by draining the batches after the sorption experiments and refilling with an equal amount of a solution free of

PFAS, and found that there was hysteresis. Johnson et al. (2007) fitted linear, Freundlich, and Langmuir isotherms for PFOS and found that all three gave acceptable results ($R^2 \geq 0.904$). For the Ottawa sand the Freundlich isotherm gave the best fit ($R^2=0.978$) and for the iron-rich sand the Langmuir isotherm gave the best fit ($R^2=0.971$). Enevoldsen et al. (2010) fitted both linear and Freundlich isotherms and found generally good fits for the former (did not report on the latter) for several PFAS. They also conducted desorption experiments and found hysteresis in the isotherms, which they say is evidence of two or more adsorption sites. You et al. (2010) fitted the Freundlich isotherm to both the sorption and desorption data for PFOS. Like the other studies that investigated desorption they also found hysteresis in the isotherms. Ahrens et al. (2011) fitted linear isotherms to their data and found good fits, which they say is expected at the low concentrations investigated. The non-ideal adsorption/desorption behaviour seen in the hysteresis of the adsorption/desorption isotherms can lead to non-ideal transport behaviour (i.e. extended elution tailing), having ramifications for modelling PFAS transport (Brusseau et al., 2019a).

Table 3 Summary of Freundlich parameters K_f and n from the literature. The linearity of some of these isotherms are (close to) linear, which could explain why several studies decided to use a linear isotherm instead.

Source	PFOA		PFOS		Comments
	K_f	n	K_f	n	
Higgins & Luthy (2006)	-	0.77-0.93	-	0.81-0.96	K_f were not reported.
Miao et al. (2017)	1.60-8.85	0.78-1.27	-	-	
Johnson et al. (2007)	-	-	50	0.555	Only fitted parameters for the Ottawa sand are shown.
You et al. (2010)	-	-	56-2570	0.51-0.69	Values include experiments at different pH's and with different $[Ca^{2+}]$.
Zhi & Liu (2018)	0.07	1.05	0.28	0.82	Only values for experiments done with peat sample are shown.
Milinic et al. (2015)	2-40	0.9-1.1	17-389	0.9-1	Includes values for several samples.
Guelfo & Higgins (2013)	0.56-1.77	0.89-1.08	2.29-12.89	0.83-0.94	

2.2.5. Field vs. Lab Derived Partition Coefficients

(39) When comparing field and lab determinations of K_d , field-derived values are consistently higher than those determined in lab batch experiments (Li et al., 2018; Zareitalabad et al., 2013). Li et al. compared the median log K_d values for PFOS, PFOA, PFNA, and PFDA and found that they were 1.6, 4.0, 1.9, and 1.7 time higher, respectively, than the mean log values derived from lab experiments. Even when K_{oc} values are compared field-derived values are larger than their lab-derived counterparts (Zareitalabad et al., 2013). However, there are some important things to consider regarding field-derived coefficients, such as the assumption that sediment and overlying water are in equilibrium seeing as overlying water is continually changing due to flow. Exactly how this leads to consistent overestimation of partitioning coefficients is not clear, though, since simply not being in equilibrium would mean also smaller partitioning coefficients for field-derived values are possible. Spatial variability can also be important as shown in Ahrens et al. (2010), who found at one sampling location significant concentration differences at different depths. However, it is possible that field K_d values are indeed higher, and Zareitalabad et al. suggest that this could be due to the lower concentrations found in natural systems and the non-linear nature of the sorption isotherms not reflected in lab batch experiments at higher concentrations. Another explanation is ageing of the soil and sorption

hysteresis, as evidenced in Enevoldsen & Juhler (2010) and Miao et al. (2017), which also generally enhances the binding of prior contamination (Zareitalabad et al., 2013).

2.2.6. Section Summary + Take-Home Message

(40) In the prior sections, various factors that influence the solid-phase adsorption of PFAAs (mostly PFOA and PFOS) were examined. When it comes to describing the adsorption process, there are two hypothetical approaches: 1) identify all the individual speciation reactions between the PFAS and the sorbent (i.e. identify the different types binding sites of the sorbent, and concentration of those sites), and quantify these reactions through reaction equations and/or equilibrium expressions, or 2) lump all the various speciation mechanisms together and describe them with a partitioning coefficient (e.g. K_d). This latter approach simplifies characterizing the adsorption process, yet it also makes it difficult to obtain a single partitioning coefficient that can be used to describe all or several systems. To acquire partition coefficients for any given system *a priori*, knowledge from the literature regarding influences on the adsorption behaviour can be useful.

(41) From the literature and discussions in the prior sections it is clear that the sorption behaviour of PFAAs is complex. Both electrostatic and hydrophobic interactions play an important role in the sorption behaviour in environmental conditions. From the literature it can be deduced that simply using K_{oc} , as is commonly done with organic contaminants, could be oversimplifying the system and not accurately describe the sorption behaviour. The use of K_{oc} implies that adsorption is controlled by OC, and while sorption to OC might be the dominant sorption process, other factors appear to have a significant enough effect to question the reliability of K_{oc} . These other factors are sorption to (clay) minerals, influence of pH, ionic strength, and cations, and non-linear isotherms. Li et al. (2018) collated a large dataset from the literature to see if any one of these factors are clearly dominant, but to no avail. Subsequently, they suggest instead to use multiple regression analysis (or principle component analysis if possible), which in their analysis generally gave better regressions and more significant relationships, albeit the sample sizes were small. However, perhaps the “safest” way would be to determine distribution coefficients of the sediments of interest experimentally, especially if the sediments are characterized by low OC content (Ferrey et al. 2012). To close off this section are two tables. Table 4 summarizes the regression data of Li et al. for PFOA and PFOS, indicating that no regression considering a single factor was able to adequately describe the spread in K_d values. The multiple regressions on the other hand did give much better fits. Table 5 shows some K_d and K_{oc} values as reported in the literature. The data therein can be used to get an idea of the spread of values of K_d (or K_{oc}), which may be useful in deriving a mean K_d . While this would be less preferred to obtaining empirical relationships between the factors mentioned in this chapter and K_d , if that is not an option then this is an alternative.

Table 4 Regression data taken from Li et al. (2018); regressions were done with K_d . Only the data for PFOA and PFOS are shown, but data for other PFAS are available. For the simple regressions only %OC was significant for both PFOA and PFOS, but the R^2 is low. Overall, the multiple regressions describe the variation in K_d much better than the simple regressions.

Property	PFOA			PFOS		
	R^2	Significance level	n	R^2	Significance level	n
%OC	0.07	0.002**	147	0.05	0.003**	178
pH	0.07	0.117	36	0.06	0.201	27
%Clay	0.04	0.317	29	0.06	0.390	15
Ca ²⁺	0.14	0.416	7	0.11	0.068	32
Na ⁺	0.08	0.582	6	0.05	0.318	23
CEC	0.07	0.298	18	0.30	0.102	10
AEC	0.46	0.063	8	0.01	0.911	4
OC + pH	0.31	0.004**	33	0.75	1.1E-6***	23
OC + %Clay	0.43	0.0007***	29	0.76	0.0002***	15
OC + Ca ²⁺	-	-	-	0.71	2.4E-7***	28
OC + Na ⁺	-	-	-	0.76	1.1E-5***	19
OC + %Clay + pH	0.45	0.002**	29	0.77	0.0008***	15

*P<0.05; **P<0.01; ***P<0.001

Table 5 K_d and K_{oc} values are in L/kg. *n refers only to the number of sediments used for determination of K_{oc} , except for the field derived methods in which case it also refers to the K_d determination. **Data from this study were given in L/g and converted to L/kg, but results are dubiously high. ***suspended particulate matter.

PFOA		PFOS		n*	Isotherm	C_{water} range [ng/L], [PFOA]:[PFOS]	Determination method	Comments	Reference
log(K_d)	log(K_{oc})	log(K_d)	log(K_{oc})						
0.67– 1.16	2.2–2.6	0.97– 1.96	3.0– 4.20	9	Linear	1.4–140	Lab		Ahrens et al. (2011)
0.17– 0.26	0.17– 0.63	1.18– 1.23	1.18– 1.6	4	Linear + Freundlich	< 600	Lab		Enevoldsen & Juhler (2010)
-	-	0.45– 0.94	2.4–2.6	3	Linear+Langmuir+ Freundlich	< $8 \cdot 10^6$	Lab	Includes SSA values	Johnson et al. (2007)
0.41– 1.08	2.11	0.26– 1.66	2.68	4	Freundlich	74–341 : 67– 221	Lab	Includes SSA values	Higgins & Luthy (2006)
2.69– 3.17	4.40– 4.97	-	-	10	Linear + Freundlich	~10000– 300000	Lab	Also measured desorption isotherms.	Miao et al. (2017)**
-0.24– 0.54	-	0.42– 1.56	-	5	Freundlich	540–286000 : 90–72730	Lab	Also looked at influence of co- contamination.	Guelfo & Higgins (2013)
1.07- 3.56	1.72- 5.19	1.33- 3.34	2.93- 5.12	125	-	0.41 – 130 : 0.52 – 350	Lab	Contains data on other PFAS along with select soil properties.	Wintersen et al. (2020b)
-0.1- 1.69	1.98	0.95- 2.64	2.85	6	Freundlich + Linear	~ 10^3 – $7 \cdot 10^3$: ~ 10^3 – $6 \cdot 10^3$	Lab		Milinic et al. (2015)
-	-	0.27- 1.37	2.97- 3.20	15	-	$5 \cdot 10^5$ – $2.5 \cdot 10^6$	Lab		You et al. (2010)
1.85- 1.95	-	2.08- 2.51		1	-	500 – 10^5	Lab		Zhi & Liu (2018)
0.04– 2.4	1.9–2.4	1.8– 2.6	3.7–3.8	6	-	~2.5–9 : 0.9– 2.2	Field	Includes data on other PFAAs and includes SPM*** data. Sampled at 2 locations.	Ahrens et al. (2010)
1.85	2.63	2.35	3.16	19	-	6.5–43 : 4.7–32	Field		Kwadijk et al. (2010)
-	3.09– 3.62	-	3.26– 3.80	47	-	8.38–25.9 : 1.78–11.3	Field	Includes SPM data and isomers of PFOA and PFOS	Chen et al. (2015)
0.69– 0.82	3.9–4.0	-	-	-	-	1.0-15.9	Column	Column experiment designed to simulate bank- filtration	Vierke et al. (2014)
0 – – 0.57	2–2.56	-1– 0.09	2.4–3.5	3	-	~ 10^6 : ~ 10^5 – 10^6	Microcosm	K_d decreased over time.	Ferrey et al. (2012)

2.3. Air-Water Interfacial Adsorption

(42) Another process that may significantly affect fate and transport of PFAS in the unsaturated zone is adsorption to air-water interfaces. PFCAs and PFSAs, and especially the longer chained compounds, have the characteristic structure of what are known as surfactants: namely a hydrophobic ‘tail’ (i.e. the fluorinated alkyl chain) and an (an)ionic ‘head’ (i.e. the deprotonated head group; carboxylate and sulfonate). As a result of this structure, and the polar nature of water molecules, surface-active compounds will tend to sit on these interfaces. Despite this, this process had not been considered in recent comprehensive reports on PFAS management (e.g. Smith et al, 2016; CRCCARE, 2017).

(43) Similar to partitioning to the solid-phases, adsorption to air-water interfaces (AWIs) can also be described using a partitioning coefficient (e.g. Costanza et al., 2019; Schaefer et al., 2019; Brusseau, 2019):

$$K_{awi} = \frac{C_{awi}}{C_{aq}} \quad (9)$$

(44) where K_{awi} is the AWI partitioning coefficient [$L^3 L^{-2}$; volume liquid/area AWI], and C_{awi} is the equilibrium concentration on the interface [$M L^{-2}$; mass compound on interface/area AWI]. Note that C_{awi} in eq. 9 is a function of C_{aq} . When the function is linear (i.e. $C_{awi} = \alpha \cdot C_{aq}$, where α is a constant), then K_{awi} is also a constant with respect to C_{aq} . This formulation slightly differs from that in Guo et al. (2020):

$$K_{awi} = \frac{C_{awi}}{A_{awi} \cdot C_{aq}} \quad (10)$$

(45) where A_{awi} is the specific AWI area [$L^2 L^{-3}$; area AWI/total volume], and C_{awi} is also the equilibrium concentration but with different units [$M L^{-3}$; mass compound on interface/total volume]. Eq. 9 and 10 say essentially the same thing; the difference is how C_{awi} is defined in terms of units by the introduction of A_{awi} . This would be analogous to:

$$C_{aq,1} = \theta \cdot C_{aq,2} \quad (11)$$

(46) where $C_{aq,1}$ is the concentration in solution defined differently in terms of units [$M L^{-3}$; mass in water/total volume], and $C_{aq,2}$ is also the concentration in solution but defined the same as in eqs. 9 and 10 (i.e. mass in solution/volume water). For clarification, the total volume is the volume of water plus the volume of air plus the volume of grains. In this report the C_{awi} is defined as in eq. 9. This is done for the sake of continuity: since both C_{aq} and C_s are described in terms of mass of compound in their respective ‘domains’ (i.e. mass of compound in water/volume water & mass of compound on solids/mass of solids) it makes sense to define C_{awi} as the mass of compound on the interface/interfacial area.

(47) Brusseau et al. (2019) and Lyu et al. (2018) demonstrated that AWI adsorption can be responsible for a significant amount of total retention for both PFOS and PFOA. They conducted miscible flow-through experiments (i.e. column experiments) at various saturations (yet homogeneous) and for steady-state conditions to determine the effect AWI adsorption. For the experiments done in a sand medium with a low solid-phase partitioning coefficient ($K_d \sim 0.15$ L/kg for PFOS), AWI adsorption accounted for $\sim 80\%$ of total retention. For the experiments done in a soil with a higher K_d (~ 0.56 for PFOS), the contribution to total retention from interfacial adsorption was less ($\sim 32\%$). However, this was also in part due to the higher initial concentration of PFOS in the experiments conducted in the soil and the non-linear relationship between concentration and interfacial partitioning coefficient (K_{awi}): at higher concentrations K_{awi} decreases, yet this will be elucidated later on. In the experiments

of Lyu et al. (2018), they found that retardation was greater for lower saturations and for smaller grain size, which they say is consistent with the impact these conditions would have on the magnitude of the air-water interfacial area (AWIA). They also found that retention was considerably greater for lower input concentrations of PFOS, which they say is consistent with the non-linear nature of surfactant fluid-fluid adsorption with respect to concentration. In any case, this shows that for certain systems, which could occur in the environment, AWI adsorption can be a significant source of retention and so should not be neglected.

(48) Brusseau et al. (2019) also developed a multi-process retention model that accounts for several potential sources of retardation in source zones, which are AWI adsorption, soil atmosphere partitioning, non-aqueous phase liquid (NAPL) – water interface adsorption, NAPL partitioning, and solid phase adsorption (fig. 6).

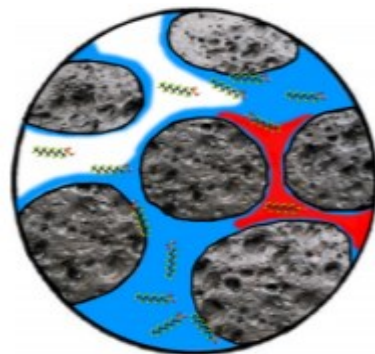


Figure 5. Illustration of the pore-scale retention processes considered in Brusseau (2018) and Brusseau et al. (2019). Squiggly lines are PFAS, white areas are air, blue are water, and red NAPL. The retention processes shown are partitioning into the 3 fluid phases, and adsorption onto the surfaces/interfaces. Image from Brusseau (2018).

(49) The porous medium properties used in the model were based on measured porous media and represent a sandy vadose-zone soil, and data from literature were used to determine partitioning coefficients. The results showed that for PFOA and PFOS the primary source for retention was adsorption at the AWI, which accounted for ~50% of the total retention, whereas solid-phase sorption accounted for 15% for PFOA and 22% for PFOS. NAPL partitioning and NAPL-water interfacial adsorption also contributed substantially to retention, combined amounting to 30% and 27% of total retention for PFOA and PFOS, respectively. When compared to each other, PFOS exhibited over three times as much retardation as PFOA ($R=14.1$ for PFOA and $=47.9$ for PFOS). The study also modelled 8:2 fluorotelomer alcohol (8:2 FTOH) and the retardation factor was much higher than that of either PFOA or PFOS ($R=9906$), with 98% of the retention being due to NAPL partitioning and virtually no retention due to adsorption to the fluid-fluid interfaces (i.e. water-air and water-NAPL). Partitioning of 8:2 FTOG to NAPL could thus be relevant when considering more heavily contaminated sites where other contaminants besides PFAS are present, such as NAPLs.

(50) Regarding the factors that control AWI adsorption, looking at eq. 9 (and 10) can give some insight. From these equations the two most important aspects are the specific AWIA (A_{awi}) and the partitioning coefficient (K_{awi}). Various influences on these factors will be discussed below. These are: the degree of saturation, PFAS concentration, and molar volume. Other factors are things like pore-size, grain-size, and soil-composition, yet these are not discussed specifically in this report.

2.3.1. Degree of Saturation

(51) The degree of saturation has direct implications for the specific AWIA, and thus also adsorption to the AWI. From the literature it is clear that as saturation increases, AWIA decreases (e.g. Kim et al., 1997 & 1999; Schaefer et al., 2000; Peng & Brusseau, 2005; Costanza-Robinson & Brusseau, 2002). To determine a relationship between the specific AWIA and saturation, results from lab experiments can be used. While several types of experimental methods to determine specific AWIA exist, most involve advective (but also diffusive) transport of an interfacial partitioning tracer (i.e. a compound that adsorbs to air-water interfaces), which can be either aqueous (e.g. Kim et al., 1997; Brusseau et al., 2015) or gaseous (e.g. Kim et al., 1999; Peng & Brusseau, 2005). Other methods include using imaging via synchrotron X-ray microtomography (e.g. Brusseau et al., 2006) and surfactant-induced water mobilization (e.g. Karkare & Fort, 1993). With the data, various empirical relationships between A_{awi} and S_w have been found. A linear fit has been reported in some studies (e.g. Kim et al., 1997; Schaefer et al., 2000; Brusseau et al., 2006), with the equation having the form:

$$A_{awi} = A_{max}(1 - S_w) \quad (12)$$

(52) Where A_{max} is the maximum specific AWIA [$L^2 L^{-3}$; area AWI/total volume], and S_w is the saturation [$L^3 L^{-3}$; volume water/volume pore-space or water-content/porosity]. However, Schaefer et al., who investigated the AWIA–water saturation relationship for both drainage and imbibition conditions using a method relying on *diffusive* transport of an aqueous surfactant, only found the linear relationship under drainage conditions. This hysteretic behaviour agrees with the expectations of Bradford & Leij (1997), who developed a theoretical model for the relationship between AWIA and saturation. In addition, as expected by Bradford & Leij, Schaefer et al. found that at a given saturation and for the same porous medium, the AWIA under drainage conditions is greater than under imbibition conditions. With respect to eq. 12, the term S_w does not have a coefficient (i.e. the slope and y-intercept are the same) because at full saturation (i.e. $S_w=1$) the AWIA should be zero. Also, the parameter A_{max} represents the maximum specific AWIA that can be achieved, and is expected to vary per porous medium (Costanza & Brusseau, 2000). While factors controlling A_{max} do not appear to be well understood yet, two correlations have been reported. Lyu et al. (2018) found an empirical relationship between the median grain diameter and A_{max} for silica sands ($n=7$, $R^2=0.97$):

$$A_{max} = 61.3 \cdot d^{-1.2} \quad (13)$$

(53) Where d is the median grain diameter [L ; in mm]. Costanza-Robinson & Brusseau (2002) found that for the aqueous-phase interfacial partitioning tracer methods (both diffusive and advective), the A_{max} is close to the specific surface area (SSA) of the porous medium as calculated using the “smooth-sphere” assumption. Furthermore, Costanza & Brusseau (2000) state that SSA is likely the key aspect of soil texture responsible for the predicted dependence of specific AWIA on soil texture seen in Cary (1994). In other words, SSA is expected to be an important factor influencing A_{awi} , and thus also A_{max} . When A_{max} is plotted against SSA (Costanza-Robinson & Brusseau, 2002), the linear regression gives an R^2 of 0.695 ($n=10$), with the fitted line being:

$$A_{max} = 0.564 \cdot SSA \quad (14)$$

(54) Where SSA is the specific surface area of the porous medium [$L^2 L^{-3}$; surface area porous medium/total volume; units of SSA in cm^{-1}]. Note that this definition of SSA is slightly different to the one in section 2.2.2. (Table 2): here the surface area of the porous medium is normalized to the volume of the porous medium, as opposed its mass. Important to recognize is that for some studies A_{max} is determined via extrapolation to $S_w=0$ (e.g. see linear regression in fig. 7), and so their validity at small water-contents/saturations is questionable. This also brings into question the validity of using eqs. 12, 13, and 14 at sufficiently low water-contents since it is not clear whether the values for A_{max} used to

determine the empirical relations (i.e. eqs. 13 and 14) were determined via extrapolation (e.g. Kim et al., 1997) or measured at small S_w (e.g. Schaefer et al., 2000).

(55) With respect to the agreement of the results for the different methods, discrepancies are evident, indicated by A_{awi} at a given water saturation being different depending on the method used. Kim et al. (1999) compared the results of the gaseous tracer method to the aqueous tracer method for the same porous medium and found that the former gave significantly higher specific AWIAs than the latter for the same saturation. Figure 7, from Kim et al. (1999), presents the two datasets together, and the difference in measured AWIA can be seen in the saturation range 0.29–0.55 (i.e. the range over which both datasets are represented). One possible reason for this is that the two methods access different interfacial domains (Kim et al., 1999; Costanza-Robinson & Brusseau, 2002). In other words, since these methods rely (mostly) on advective transport of either gas or water, they likely underestimate the interfacial area at low saturation of the respective fluids. This is because at low saturation of either air or water, there will be isolated pockets of the respective fluid that do not contribute to advective flow. As such, Costanza-Robinson & Brusseau say that the two methods are complimentary in that they are most applicable at different water saturations. Simultaneously, however, since PFOA and PFOS are not expected to be in the vapour phase in the environment, using empirical relationships based on gas-phase method may overestimate the magnitude of *effective* AWIA for contaminants in solution. As such, for a worst-case scenario in which the mobility of PFAS is maximal it is advised to use a linear relationship between A_{awi} and saturation as determined by the aqueous-phase methods since using such a model would give the lowest physically relevant values for A_{awi} .

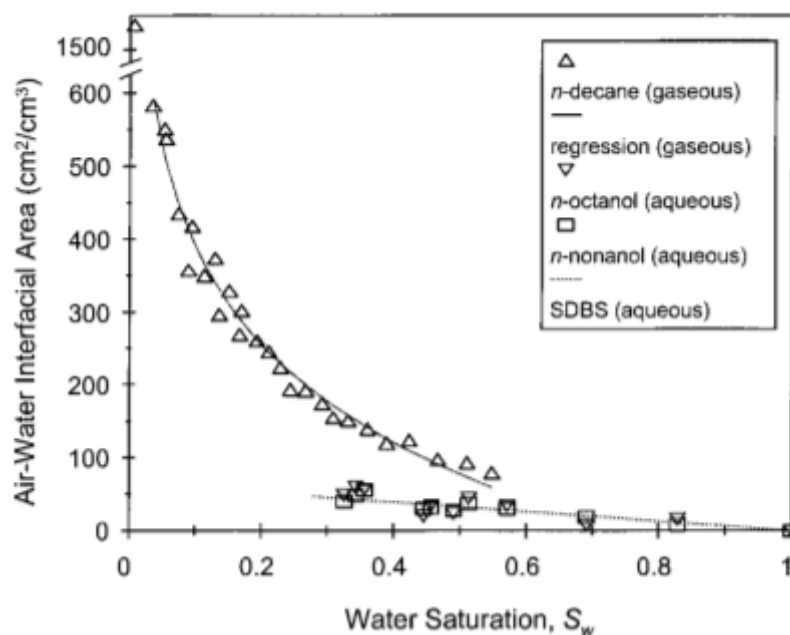


Figure 6 Data from Kim et al. (1999) in which the specific air-water interfacial area is plotted vs. water saturation. Data from two methods are shown: one using a gas-phase interfacial partitioning tracer (*n*-decane), and one using a liquid-phase interfacial partitioning tracer (octanol and SDBS). The results show that the two methods not only show different trends, but also give different magnitudes for A_{awi} at a given saturation. The regression line through the *n*-decane data is a log fit [$A_{awi} = 196 \cdot \ln(S_w) - 58.9$, with $R^2=0.978$]. Image from Kim et al. (1999).

(56) Aside from the difference in measured A_{awi} , the trends are also different: the gas-phase method shows an exponential increase in specific AWIA while the aqueous method shows a linear increase, with decreasing water saturation. This exponential increase in A_{awi} with decreasing water saturation

for the gas-phase method was also seen in Peng & Brusseau (2005) for 6 different porous media. They also used a function of identical form to the van Genuchten equation describing the soil-water retention characteristic, which incorporates two fitting parameters. Analysis of the fitted values of these parameters for the 6 different media revealed that both parameters correlate to the uniformity coefficient, which is an index for particle size distribution of a porous medium. They used this empirical model to simulate the results of Kim et al. (1997 & 1999), and the model was able to predict the data reasonably well. For the sake of brevity, the model is not elaborated on in this report, yet a comprehensive description of the model can be found in Peng & Brusseau (2005).

(57) The degree of saturation clearly has an important role in describing adsorption to the air-water interface, since it is closely linked to the magnitude of AWIA. The precise nature of the relationship is not clear yet. Results from experiments suggest both linear and exponential relationships are valid, depending on the type of method used in determining the AWIA. With respect to modelling transport of surfactant PFAS in unsaturated conditions, it is not clear what model would be best. On the one hand, it seems intuitive to only use data/models for the methods employing transport of aqueous surfactants, since these PFAS (i.e. PFOA and PFOS) will also be introduced into the soil via the aqueous phase. On the other hand, perhaps using the data from the gas-phase method is better since this method is assumed to give results that better reflect *total* AWIA, especially at low saturation. This may also be desired since it's not clear what the effect of multiple drainage and imbibition cycles will have on the magnitude of effective AWI, as it may be that the effective AWIA is greater than anticipated by the aqueous tracer methods under these conditions (i.e. conditions of multiple drainage and imbibition cycles). Furthermore, although not discussed here, there also exist theoretical models that describe the relationship between saturation and AWIA (e.g. Bradford & Leij, 1997). These approaches are quite complex and difficult to follow, yet the predicted magnitudes of A_{awi} from Bradford & Leij are comparable to those determined by the aqueous tracer method. For that reason, under the *worst-case* assumption it is advised to use either the linear model as determined from the aqueous-phase methods or theoretical models which give similar magnitudes for A_{awi} , as these values will predict increased mobility of surfactant PFAS.

2.3.2. Surfactant Concentration

(58) Similar to solid-phase adsorption, PFAS adsorption to the AWI is also a function of PFAS concentration. In other words, isotherms can be used to describe the process of adsorption to the AWI. The isotherms reported in the literature are the linear, Freundlich, and Langmuir isotherm, and the appropriate isotherm depends on the concentration range in question. To determine the relationship between interfacial concentration and aqueous concentration, surface tension data is commonly used. The equilibrium surface concentration (C_{awi}) as defined in eq. 9 (section 2.3.; i.e. mass compound on interface/area AWI), commonly referred to as *surface excess* in the literature, can be described using the Gibbs equation (Costanza et al., 2019; Schaefer et al., 2019; Brusseau, 2019), which relates the surface excess to the surface tension of a solution:

$$C_{awi} = -\frac{C_{aq}}{R \cdot T} \cdot \frac{\partial \gamma}{\partial C_{aq}} \quad (15)$$

(59) where R is the universal gas constant, T is the temperature, and γ is the surface tension [M T⁻²; force/length]. In turn, the surface tension of a solution can be described using the Szyszkowski equation (Costanza et al., 2019; Schaefer et al., 2019; Brusseau et al., 2019; Guo et al, 2020):

$$\gamma = \gamma_0 \left[1 - a \cdot \ln\left(\frac{C_{aq}}{b} + 1\right) \right] \quad (16)$$

(60) where γ_0 is the surface tension of pure water [$M T^{-2}$; force/length], and a [-] and b [$M L^{-3}$; surface activity] are fitting parameters. Substituting eq. 16 into eq. 15 and differentiating with respect to C_{aq} gives the following isotherm:

$$C_{awi} = \frac{a \cdot \gamma_0}{R \cdot T} \cdot \frac{C_{aq}}{C_{aq} + b} = C_{awi_max} \cdot \frac{C_{aq}}{C_{aq} + b} \quad (17)$$

(61) This isotherm is known as the Langmuir isotherm, and suggests that at large enough concentrations (such that $C_{aq} \gg b$) the interface gets saturated and a maximum surface concentration/excess is reached. This maximum concentration is described by the first term ($a \cdot \gamma_0 / R \cdot T$). When looking at the partitioning behaviour (K_{awi} ; eq. 9, section 2.3.), eq. 17 suggests that as C_{aq} increases K_{awi} decreases, and approaches zero as C_{aq} approaches infinity. Conversely, at low concentrations (such that $b \gg C_{aq}$), the isotherm becomes linear and as such a maximum (and constant) partitioning coefficient is reached, described by $(a \cdot \gamma_0) / (R \cdot T \cdot b)$. By fitting surface tension data from multiple sources to eq. 16, Brusseau (2019) found that for most of the PFASs he studied (including PFOA and PFOS) the PFAS concentration below which K_{awi} is constant and maximal is around 0.1 mg/L. For PFOA and PFOS the maximal K_{awi} (i.e. at concentration of 0.1 mg/L) are **2.32E-04 cm** and **2.30E-3 cm**, respectively. It should be noted, however, that these values were determined for a pure water solution (i.e. without any ions in solution). In a solution with other ions, as is the case in natural soil-water and groundwater, surface activity of surfactants increases (Brusseau 2019).

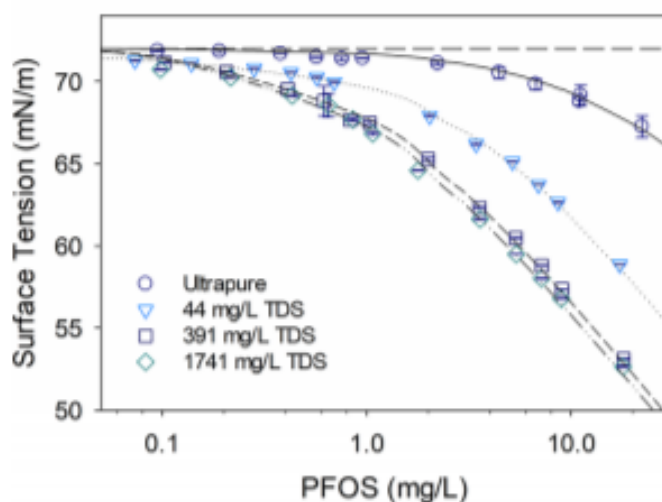


Figure 7 Data of Costanza et al. (2019) showing the surface tension data for K-PFOS in solutions containing different amounts of TDS. The fitted lines were made using the Szyszkowski equation (eq. 16), indicating that at these concentration ranges the equation adequately describes the relationship between surface tension and PFOS concentration. Image from Costanza et al. (2019).

(62) To address the influence of ions in solution, Costanza et al. (2019) measured the surface tension at various PFOA and PFOS concentrations for four different solutions with varying concentrations of total dissolved solids (TDS; ranging from pure water to ~1700 mg/L TDS). They fitted the Szyszkowski equation to the data for the 4 solutions (see fig. 8 above) and found average maximum interfacial concentrations and an empirical relationship between the surface activity (b in eqs. 16 and 17) and TDS. The data are summarized in table 6 below. The reported average values for C_{awi_max} and correlations between TDS and surface activity are valid within the reported PFOA and PFOS

concentration ranges (0.1-25 mg/L for PFOA and 0.1-90 mg/L for PFOS) and the TDS concentration range (ultrapure to 1700 mg/L).

Table 6 Summary of fitted parameters for the experiments done in Costanza et al. (2019). The fitted values are valid **only** for the PFOA and PFOS concentration ranges, and the TDS concentration range.

Solution	Compound & fitted concentration range			
	PFOA: 0.1 to 25 mg/L		PFOS: 0.1 to 90 mg/L	
	Maximum surface excess [mg/m ²]	Surface activity (b) [mg/L]	Maximum surface excess [mg/m ²]	Surface activity (b) [mg/L]
Ultrapure	0.38 ± 0.2	14.7 ± 9.4	1.28 ± 0.15	18.4 ± 3.8
ca. 40 mg/L TDS	0.41 ± 0.08	4.8 ± 1.6	1.47 ± 0.04	3.5 ± 0.3
ca. 400 mg/L TDS	0.63 ± 0.07	3.5 ± 0.7	1.39 ± 0.02	1.1 ± 0.1
ca. 1700 mg/L TDS	0.63 ± 0.04	2.7 ± 0.4	1.36 ± 0.02	1.0 ± 0.1
Average/correlation	0.51 ± 0.32	(8.58±0.21)·TDS ^(-0.152±0.005)	1.37 ± 0.16	(9.07±2.6)·TDS ^(-0.32±0.06)

(63) While the values for K_{awi} and isotherm parameters reported in Brusseau (2019) and Costanza et al. (2019) are useful for concentration ranges above 0.1 mg/L, the behaviour of C_{awi} at lower aqueous concentrations of PFAS is uncertain since it is not possible to measure changes in the surface tension reliably at low PFAS concentrations (i.e. measurable changes in surface tension only occur at greater concentrations; Schaefer et al., 2019). As such, Schaefer et al. developed a novel method to measure PFAS partitioning to the AWI at lower concentrations which does not rely on interfacial tension measurements. They used data from this method, along with interfacial tension measurements, for PFAS in solutions with NaCl and found that a Freundlich (as opposed to Langmuir) isotherm best described the relationship between C_{awi} and C_{aq} across the entire concentration range investigated (spans ~7 orders of magnitude for PFOS: 10^0 - 10^{-6} mol m⁻³), with the equation having the form:

$$C_{awi} = k \cdot (C_T)^n \quad (18)$$

with

$$C_T = C_{aq} \cdot (C_{aq} + C_{NaCl}) \quad (19)$$

(64) where k and n are the Freundlich fitting parameters, C_T is the square of the mean ionic activity [(M L⁻³)²], and C_{NaCl} is the background NaCl concentration [M L⁻³]. The interfacial surface tension measurements, which were done at higher PFAS concentrations than the novel method, were used to determine the fitting parameters (i.e. k and n), with good fits being found for all tested systems ($R^2 > 0.98$; see also table S1 in supporting information of Schaefer et al., 2019). The fits were also extrapolated to the lower concentrations of the alternative method, and were found to agree reasonably (see fig. 9). Also plotted in figure 9 is the Langmuir isotherm (dashed line), and it is clear that using this isotherm to describe partitioning of PFOS at the AWI will drastically underestimate the magnitude of adsorption to the AWI at the lower concentrations (10^{-6} mol m⁻³ = 500 ng L⁻¹). This has important implications when considering adsorption to the AWI during transport at these low concentrations, namely that more retardation is expected to occur than when assuming the maximum K_{awi} as predicted using the Langmuir isotherm. Similar results were found for PFOA. The fitted parameter values for PFOA and PFOS (and other PFCAs and PFSAs) can be found in table S1 in the supplementary information of Schaefer et al. (2019).

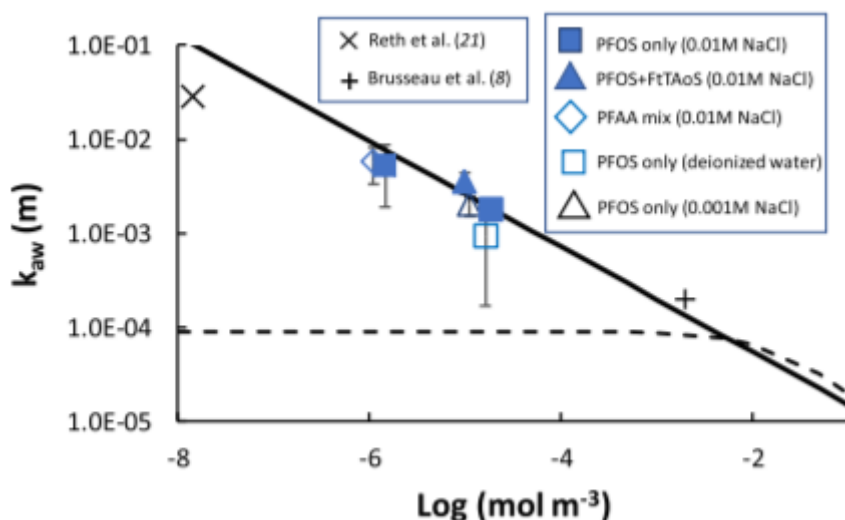


Figure 8 Data from Schaefer et al. (2019), plotting K_{ow} vs. $\log([PFOS])$. The solid regression line was determined from the Freundlich isotherm fit of the interfacial tension data of PFOS in 0.01 M NaCl solution (not shown), with the values of the Freundlich parameters being: $k=1.5(\pm 0.2) \cdot 10^{-6}$ and $n=0.44(\pm 0.08)$, with $R^2=0.99$. The dotted line is the fit of Langmuir isotherm for the same dataset (i.e. interfacial tension data of PFOS in 0.01 M NaCl solution; not shown). From this one can see that using the Langmuir isotherm underestimates K_{ow} for PFOS at concentrations below $\sim 10^{-2} \text{ mol m}^{-3}$. Image taken from Schaefer et al. (2019).

(65) With all this being said, when it comes to modelling transport of PFOA and PFOS in the unsaturated zone while accounting for adsorption to the AWI, the following suggestions are made regarding choosing the appropriate adsorption model and parameter values. When the concentration of PFOA or PFOS in the soil water is expected to be above 0.1 mg/L, then use of the Langmuir isotherm and associated parameter values from Costanza et al. (2019) is suggested. This is because the empirical equation relating the TDS to the surface activity (parameter b in eq. 17) can be used to account for the effect of ions in solution on K_{ow} . If concentrations are expected to be below 0.1 mg/L, then application of the Freundlich isotherm and associated parameter values reported in Schaefer et al. (2019) are advised since they would better approximate the expected retention due to adsorption at the AWI. Alternatively, use of the Langmuir isotherm of Costanza et al. (2019) or the K_{ow} reported in Brusseau (2019) for a PFAS concentration of 0.1 mg/L is also valid under the assumption of a worst-case scenario. This is because it is expected that using these values for K_{ow} would overestimate the mobility of these compounds, meaning they would have a greater impact on the underlying groundwater.

2.3.3. Molar Volume

(66) Like with the solid-phase partitioning coefficients, Brusseau (2019) looked at the relationship between numerous (compound) structure properties and fluid-fluid interfacial adsorption coefficients (e.g. K_{ow}) for a host of PFASs and some hydrocarbons through QSPR analysis. The full list of the interfacial adsorption coefficients used can be found in the study. He found that the best descriptor was the molar volume. The regression had an R^2 of 0.94, with each additional unit of molar volume (cm^3/mol) contributing 0.021 log units. However, it should be noted that most of the collated surface tension data used to determine K_{ow} was for deionized water. In reality, the presence of salts is known to increase surfactant surface activity, and so the values he reports should be considered conservative when compared to environmental conditions (i.e. they will adsorb more readily in environmental conditions). Furthermore, the data set were based on single solute systems, and so the presence of co-contaminants is also expected to have an effect. Brusseau & Van Glubt (2019) extended the QSPR

analysis to also include more environmentally realistic solutions (i.e. including ions), and used this new data to revise the regression between molar volume of PFAS and K_{awi} (see fig. 10).

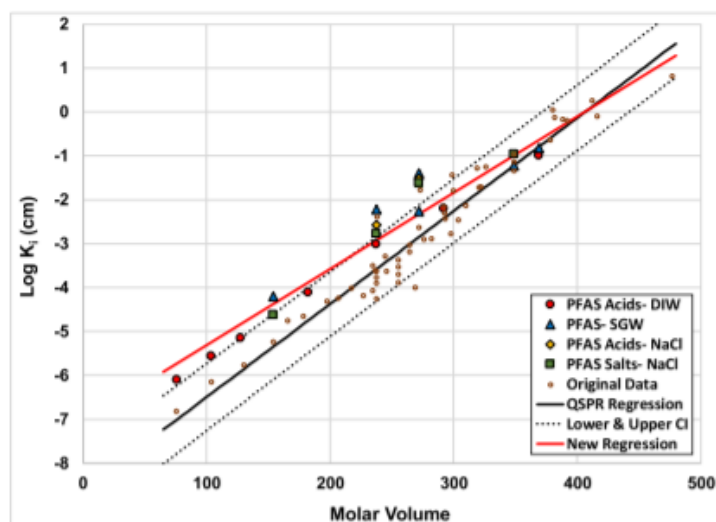


Figure 9 Graph showing results of the QSPR analysis for K_{awi} of several PFAS and hydrocarbon surfactants. Target concentration was 0.1 mg/L. Several regressions are shown; the black solid line (and dashed lines) are the original regressions in which objective K_{awi} values were determined for deionized water, and thus did not consider the effect of ionic strength on K_{awi} . The new regression (red line) was done for K_{awi} values in which solutions had dissolved salts, but also for original data for which $V_m > 300$ since the effects of ions in solution was minimal for these compounds. The regression equation is: $\log(K_{awi}) = 0.0174(\pm 0.0015) \cdot V_m - 7.05(\pm 0.4)$, with $R^2 = 0.95$. DIW = deionized water, SGW = synthetic groundwater, and NaCl denotes 0.01 M NaCl solution. Image from Brusseau & Van Glubt (2019).

(67) Schaefer et al. (2019) also looked at the relationship between molar volume and K_{awi} for the tested PFCAs (C3-C7) and PFSA (C4, C6, & C8) and found a similar trend (fig. 11). The two regressions (i.e. fig 10 and fig. 11) are complimentary in the sense that they were made with different target concentrations. In other words, to make these regressions K_{awi} needs to be known, and since they are a function of PFAS concentration a target concentration needs to be established so that a comparison between PFASs can be made. For the regression in Brusseau & Van Glubt the target concentration was 0.1 mg/L, whereas for Schaefer et al. the target concentration was $2 \cdot 10^{-6} \text{ mol m}^{-3}$, which corresponds to concentration of $\sim 280 \text{ ng/L}$ (PFBA) to $\sim 1000 \text{ ng/L}$ (PFOS). As such, depending on the expected concentration ranges either empirical relationship can be used to estimate K_{awi} .

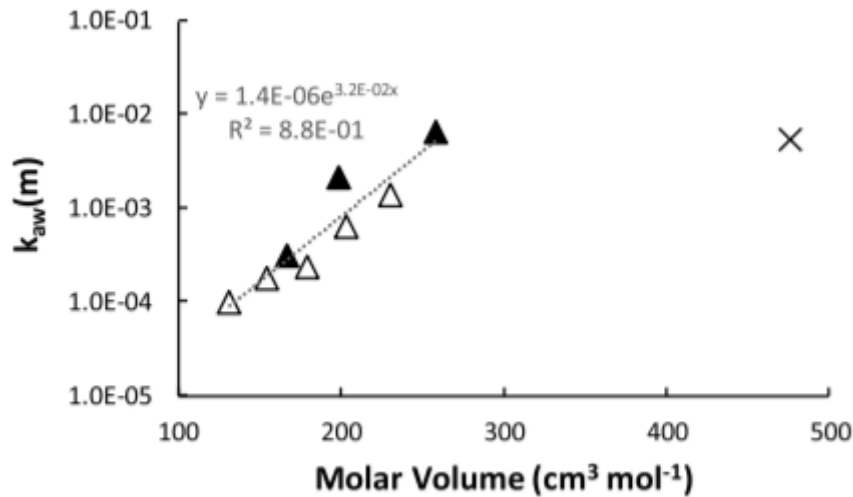


Figure 10 Graph showing regression between K_{awi} and V_m as reported in Schaefer et al. (2019), with target concentration being $2 \cdot 10^{-6} \text{ mol m}^{-3}$, which corresponds to a concentration of $\sim 280\text{-}1000 \text{ ng/L}$, depending on the PFAS. Filled triangles are PFASs and empty triangles are PFCAs. The X is FtTAoS, a compound with a very different structure (was not used in the regression). Image from Schaefer et al. (2019).

2.3.4. Section Summary + Take-Home Message

(68) To summarize the process of adsorption to the AWI, there are several things to consider. When it comes to characterizing this process, use of a partitioning coefficient (i.e. K_{awi}) can be used (e.g. Brusseau et al., 2019; C, which describes the ratio of the equilibrium concentration on the AWI and the equilibrium concentration in solution. In addition, the specific AWIA (A_{awi}) is also very important as it describes the available surface area for adsorption.

(69) The key factor that controls A_{awi} is the degree of saturation (S_w). From experiments it has been shown that as saturation increases, A_{awi} decreases. This is consistent regardless of the method used, and is also consistent with the theoretical models that exist. However, discrepancies in the literature arise when looking at the relationship between A_{awi} and S_w . Here, only experimental data was investigated. From the experiments in which an aqueous phase partitioning tracer was used to determine A_{awi} , a linear relationship was found between A_{awi} and S_w . This relationship requires a single parameter (A_{max} ; value of A_{awi} at vanishingly small S_w), which is a parameter unique per porous medium. Two empirical functions are reported to determine A_{max} from either median grain-diameter (only valid for silica sands) or the SSA of the porous medium as determined from the smooth-sphere assumption. The experiments employing transport of a gaseous interfacial partitioning tracer generally give considerably higher values for A_{awi} when compared to the aqueous phase methods, and indicate a non-linear relationship between A_{awi} and S_w . Although not discussed in depth, theoretical models to describe the A_{awi} - S_w relationship do exist, and the magnitude of the values for A_{awi} from these models are generally close to those of the aqueous phase methods. Considering this, for the *worst-case* (i.e. increased mobility of PFAS in the unsaturated zone) it is advised to use either the linear A_{awi} - S_w relationship or the relationships as determined by the theoretical models since these will give values of A_{awi} which are on the low end of the spectrum.

(70) The key factor controlling K_{awi} is the surfactant PFAS concentration. From the literature, both Langmuir and Freundlich isotherms have been shown to describe the equilibrium behaviour of surfactant PFAS. This is true for pure-water systems and solutions with ions. The Langmuir isotherm is only applicable for PFAS concentrations above 0.1 mg/L, whereas the Freundlich isotherm is applicable

for concentrations lower than 0.1 mg/L (but also greater). However, as a *worst-case* assumption the Langmuir isotherm may also be used at concentrations below 0.1 mg/L (which translates to a constant K_{aw} , i.e. linear isotherm) since this would predict increased mobility of the surfactant PFAS. Besides concentration, other factors that influence K_{aw} are other ions in solution and molar volume of the surfactant PFAS. Empirical relationships relating molar volume to K_{aw} have been reported and were done for solutions containing other ions (i.e. not pure-water), meaning that they also take the effect of ionic strength into consideration. The two empirical relationships are complimentary since they were done at two different target concentrations; one at 0.1 mg/L and the other at ~280-1000 ng/L.

(71) Other things to consider, yet not discussed or investigated, are the kinetics of adsorption to the AWI. By only using the partitioning coefficient (i.e. without using any kinetic descriptions) it is implied that adsorption to the AWI is instantaneous. It is not clear yet whether this assumption is valid, and assuming this also deviates from the *worst-case* assumption since kinetically controlled (i.e. rate-limited) retention processes or mechanisms essentially increase mobility.

2.4. (Bio)degradation

(72) The last process to discuss is (bio)degradation. With respect to PFOA and PFOS, the literature is quite suggestive that they do not degrade in any natural environments, not through biodegradation (aerobic or anaerobic), photolysis, or hydrolysis (OECD, 2002; de Voogt, 2010). In microcosm experiments (Ferrey et al., 2012) that lasted 740 days there was also no evidence of PFOA or PFOS degradation. However, PFOA and PFOS precursors do degrade in natural environments. One such precursor are FTOHs, whose degradation has been studied extensively due to their high-volume production and complex metabolism (de Voogt, 2010). While the precise metabolic pathway to PFOA is uncertain, PFOA has been found in all 8:2-FTOH degradation studies. Precursors to PFOS are N-alkyl perfluorooctane sulphonamide derivatives (e.g. N-EtFOSA), which has been shown to degrade to PFOS in activated sludge (parent product is N-ethyl perfluorooctane sulphonamidoethanol, N-EtFOSE; de Voogt, 2010). Fluorinated polymers can also contain unreacted precursors that could act as a source for PFOA and PFOS, and while no degradation studies of fluorinated polymers have unquestionably shown that they can degrade, it is expected that should cleavage of ester functions in the polymers occur then this would result in free-FTOH, which would subsequently degrade to PFCAs (de Voogt, 2010). Nevertheless, for transport of PFOA and PFOS in the unsaturated zone it appears as though degradation is not a process that needs to be considered

2.5. Conclusions

(73) In conclusion, the review of the literature has revealed three key processes which together are expected to adequately describe transport of surfactant PFAS (e.g. PFOA and PFOS) in the unsaturated zone. They are transport processes (i.e. advection, dispersion, & diffusion), adsorption to solid surfaces, and adsorption to air-water interfaces. For the two main PFAS of interest, PFOA and PFOS, (bio)degradation does not seem to be an important process, and so can be neglected. A mathematical and quantitative description of all these processes is given, along with important factors that influence them.

(74) For the transport processes, the conventional way to describe them is with the advection-dispersion equation. This equation (i.e. eq. 1, section 2.1.), or some variation of it that includes terms for other processes like adsorption, is a governing equation in most major solute transport models for transport in porous media (e.g. PEARL, SWAP, HYDRUS, PHREEQC). Integral to solving the ADE numerically are the flow conditions, namely the velocity field (i.e. $v(z)$) and the water-content profile (i.e. $\theta(z)$), along with the dispersion and diffusion coefficients. Dispersion and diffusion serve to

attenuate transport of a compound due to mixing with resident water, and since the dispersion coefficient is a linear function of the velocity (eq. 2, section 2.1.), velocity also serves to attenuate transport. In other words, these processes serve to reduce the peak concentration of PFAS at the groundwater table in the context of a fixed mass input of PFAS at the surface. The velocity and water-content profiles are dependent on infiltration rate, depth to groundwater table, and the soil-hydraulic properties (i.e. soil-water retention curve & hydraulic conductivity). As such, in any given area or region, such as the whole of the Netherlands, the vertical velocity field and water-content profile will vary in both space and time. This has ramifications for describing the “average Dutch situation”, as will be discussed in chapter 4.

(75) The process of adsorption to solid surfaces for various PFAS, and especially PFOS and PFOA, has been researched extensively. When it comes to describing the adsorption process, which also attenuates transport, two general approaches can be taken. One is to setup a speciation model in which all interactions/mechanisms between the PFAS compound and various surface sites are described via kinetic and/or equilibrium reactions equations. The other is to use partitioning coefficients and isotherms which essentially lump all the various mechanisms into a reduced number of parameters. The first method (i.e. a speciation model) lies outside the scope of the research, and thus was not investigated. However, considering the novelty of the research regarding PFAS it is expected that insufficient information is available to adequately describe adsorption in this way. This is nonetheless mere speculation since the literature was not searched for this purpose. The second method was investigated instead and simplifies the description of the adsorption process due to the reduced number of parameters required. However, it presents complications since the partitioning coefficient of a compound will surely vary in space. This is because the partitioning behaviour is dependent on a multitude of factors that may vary both geographically and in depth at any given location. From the literature it is evident that the adsorption of PFAS (and especially PFOA and PFOS) on natural sediments is quite complex, with several factors seemingly having enough of an impact that no single factor appears dominating. This brings into the question the validity of using a partitioning coefficient like K_{oc} , which is commonly done for other organic compounds, as this implies that organic carbon is the primary factor controlling adsorption. Considering this, a multiple regression analysis is suggested to consider the effect of multiple factors. The only study in which this was done is Li et al. (2018), yet the sample size for the multiple regression analysis was generally quite small, and the actual regressions were not reported. This could thus be considered a knowledge gap, as a multiple regression analysis would be beneficial in describing the partitioning behaviour for a given soil profile *a priori*. The data from the recently done batch experiments of the RIVM could be used to this effect.

(76) The final process that is expected to be important for transport of PFOA and PFOS in the unsaturated zone is adsorption to the air-water interface (AWI). Like with adsorption to solid surfaces, adsorption to the AWI is a retention process that will attenuate transport. The two aspects that are important to consider when describing adsorption to the AWI are the specific surface area of the AWI (A_{awi}) and the partitioning coefficient (K_{awi}). This first variable is a function of water saturation, and decreases as saturation increases, as evidenced in all studies investigated. Various empirical relationships have been reported in the literature, and the nature of the relationship depends on the method used to determine the A_{awi} . The linear relationship, which requires a single parameter (A_{max}) that is dependent on soil-properties, is the most straightforward and generally gives lower values for A_{awi} when compared to the other empirical relationships. In that sense, it could be used under the assumption of a worst-case scenario since using low values for A_{awi} will reduce the impact of adsorption to the AWI, and thus decrease the amount of attenuation. As for K_{awi} , like with solid-phase adsorption, its value is dependent on the aqueous concentration of the PFAS. Freundlich, Langmuir, and linear isotherms are all reported in the literature, depending on the concentration range. At

concentrations below 0.1 mg/L, a linear isotherm is predicted based on the Langmuir isotherm. However, there is evidence to suggest that the Freundlich isotherm better describes the partitioning behaviour across the “entire” concentration range (i.e. from concentrations as low as 500 ng/L to as high as 500 mg/L). Nevertheless, under the worst-case assumption the constant value for K_{awi} at concentrations below 0.1 mg/L can be used, as this will give essentially minimum values for K_{awi} at these lower concentrations when compared to the Freundlich isotherm. Alternatively, instead of relying on isotherms and parameterization thereof, the two empirical relationships relating the molar volume of the PFAS (mostly PFAAs) to the K_{awi} can be used. Each of these regressions was done at a different target concentration: one at 0.1 mg/L and the other at ~280-1000 ng/L depending on the PFAS. As such, these equations give a single value for K_{awi} which are valid for a specific concentration (i.e. the target concentration). In that sense, the two regressions are complimentary since they can be applied at two different concentration ranges. Regardless, several options to describe adsorption to the AWI are available. A decision on which option to use can be made based on the worst-case assumption, since this will give the greatest impact on the groundwater (i.e. reduced attenuation). One knowledge gap is the lack of kinetic data, implying that adsorption to the AWI can only be considered to instantaneously be in equilibrium. This deviates from the worst-case assumption since a rate-limited retention process inherently reduces attenuation when compared to assuming instantaneous equilibrium.

(77) Considering the information gathered on these three processes (i.e. transport, adsorption to solids, & adsorption to AWIs), several options to describe these processes have been found in the literature, and knowledge gaps identified. In following chapters, these processes will be synthesized into a single equation which describes transport of surfactant PFAS (chapter 3), and will be discussed in the context of describing the “average Dutch situation” (chapter 4).

3. Mathematical Framework

(78) Now that the main processes have been delineated and elucidated, the mathematical framework to describe transport of PFAS in the unsaturated zone can be pursued. Most transport models, whether they are for the unsaturated zone (e.g. PEARL, SWAP, HYDRUS) or saturated zone (e.g. MT3DMS), employ an ADE akin to eq. 1 (section 2.1.), but that likely also takes into consideration adsorption to solid surfaces (kinetic and/or equilibrium) and other terms to represent decay and sources/sinks. While the common formulations are adequate to model PFAS transport in the saturated zone, no existing public models are suitable for modelling transport of surface active PFAS such as PFOS and PFOA in the unsaturated zone. The reason for this is that there is an additional retention process that is not common for most solutes and thus not accounted for in the model governing equations, namely adsorption to fluid-fluid interfaces (e.g. air-water). As discussed previously (section 2.3.), Brusseau et al. (2019) and Lyu et al. (2018) showed via experiments that AWI adsorption can be responsible for a significant portion of total retention for both PFOS and PFOA for environmentally relevant conditions. As a result, not considering interfacial adsorption can lead to an underestimation of retardation, and thus residence time. This implies that more retardation is expected than has been assumed thus far.

(79) To derive an appropriate mathematical framework, the various processes and mechanisms influencing fate and transport of PFOS and PFOA need to be considered (chapter 2). To reiterate, for these two PFAAs, partitioning into the gas-phase is not expected to occur due to the low vapor pressure (OECD, 2002; EPA, 2002; Ding & Peijnenburg, 2013), and so this process does not need to be considered. However, precursor PFAS to PFCAs (like PFOA), namely the fluorotelomer alcohols

(FTOHs), are volatile, and so if their transport is being simulated then their partitioning into the air also needs to be considered. Similarly, PFOA and PFOS are not expected to degrade under any environmental conditions, yet precursor compounds like FTOH and N-EtFOSE do degrade under environmental conditions (e.g. activated sludge, aerobic conditions; de Voogt, 2010). So, if transport of precursor compounds is being modelled then degradation should be considered. Other relevant processes inherent to solute transport in porous media are advection, dispersion, and diffusion. Along with adsorption to the solid-phases and AWIs, this leads to the following mass-balance equation, which is the advection-dispersion equation (ADE) for a compound that adsorbs to both solids and AWIs:

$$\frac{\partial(\theta \cdot C)}{\partial t} + \frac{\partial(\rho_b \cdot C_s)}{\partial t} + \frac{\partial(A_{awi} \cdot C_{awi})}{\partial t} = -\frac{\partial(\theta \cdot v \cdot C)}{\partial z} + \frac{\partial}{\partial z} \left(\theta \cdot D \cdot \frac{\partial C}{\partial z} \right) \quad (20)$$

(80) Where θ is the water-content [$L^3 \cdot L^{-3}$; volume liquid/total volume], C is the concentration in solution [$M \cdot L^{-3}$; mass of compound in solution/volume liquid], t is time [T], ρ_b is the bulk density [$M \cdot L^{-3}$; mass soil/total volume], C_s is the concentration in solid phase (i.e. adsorbed on soil) [$M \cdot M^{-1}$; mass of compound adsorbed on soil/mass of soil], A_{awi} is the specific air-water interfacial area [$L^2 \cdot L^{-3}$; total interfacial area/total volume], C_{awi} is the concentration on the interface [$M \cdot L^{-2}$; mass of compound on interface/total interfacial area], v is the velocity [$L \cdot T^{-1}$], z is the depth [L], and D is the dispersion coefficient [$L^2 \cdot T^{-1}$]. Important to note is that A_{awi} is a function of θ , and so this relationship would need to be defined. If the concentrations on the soil (C_s) and the air-water interface (C_{awi}) are assumed to be instantaneously in equilibrium with the concentration in solution, then partitioning coefficients can be introduced and eq. 1 (section 2.1.) can be rewritten to:

$$\frac{\partial(\theta \cdot C)}{\partial t} + \frac{\partial(\rho_b \cdot K_d \cdot C)}{\partial t} + \frac{\partial(A_{awi} \cdot K_{awi} \cdot C)}{\partial t} = -\frac{\partial(\theta \cdot v \cdot C)}{\partial z} + \frac{\partial}{\partial z} \left(\theta \cdot D \cdot \frac{\partial C}{\partial z} \right) \quad (21)$$

(81) Where K_d is the solid-phase partitioning coefficient [$L^3 M^{-1}$; concentration solution/concentration solid], K_{awi} is the AWI partitioning coefficient [$L^3 L^{-2}$; concentration/total interfacial area]. Eq. 21 is identical to eq. 12 in Guo et al. (2020), with the exception that in that study a Freundlich isotherm is considered for the solid-phase adsorption as opposed to the linear isotherm assumed here. Eq. 20 and 21 thus provide a mathematical framework for modelling transport of surfactant PFASs like PFOA and PFOS in the unsaturated zone, given sufficiently low concentrations. At high concentrations surfactant-induced flow (Henry and Smith, 2003) may need to be considered, yet Guo et al. (2020) found through their simulations that considering this phenomenon did not alter their results much, even for input concentrations of PFOS as high as 1000 mg/L. Thus, if these equations are coupled to a flow model such as HYDRUS-1D or SWAP, then a robust model will be created capable of simulating diverse scenarios characterized by transient conditions.

4. Scenario Characterization

(82) When it comes to scenario characterization for modelling, it is important to discuss the context. The context here is the evaluation or determination of suitable criteria of PFAS (specifically PFOA and PFOS) in surface-applied soil/sediment in the Netherlands, with the goal of protecting the groundwater. From this stems the idea of the “average Dutch situation”, since the results need to be applicable to the Netherlands in a general sense. Naturally, many kinds of soil profiles exist within the Netherlands, with differing soil-hydrological properties and binding properties (i.e. differences in factors that affect adsorption). Also, other important aspects that vary in space are the amount of infiltration and the depth to the groundwater table. This means that the transport of surfactant PFAS

to the groundwater, and amount of attenuation during transport, will vary geographically in the Netherlands. These differences should be considered in the characterization of a scenario, or set of scenarios, such that the results apply to the “average Dutch situation”.

(83) Aside from describing the “average Dutch situation”, different options are available in describing the hydrology and chemistry of the system. The advantages and disadvantages of these approaches will be discussed.

4.1. Hydrology of the System

(84) As discussed earlier (see section 2.1.), a description of the hydrology of the system is of paramount importance when wanting to model transport in the unsaturated zone since it facilitates transport. Specifically, what is important is the velocity field (i.e. velocity as a function of depth) and water-content profile. From Spijker et al. (2009) and Verschoor et al. (2006), two general approaches to determine these two aspects can be found. These will be described in the context of describing the flow conditions for the average Dutch soils.

(85) Spijker et al. simplified the hydrology of the system by assuming steady-state water-content profiles for three ‘typical’ Dutch soils: sandy, clayey, and peaty. These water-content profiles, along with other profile data (e.g. pH, clay-content, and more), were obtained from the STONE database, and are based on analysis of field samples of the respective soil types. While special care was taken in the determination of these profiles such that they can be considered as representative for the respective soil types, uncertainty still exists in the actual representativeness of the soil types (Spijker et al., 2009). For one, it is not clear whether the typical water-content profiles are averages over a long period of time or measured in a short time window. This is important because Spijker et al. used the average infiltration rate (~300mm/yr; period over which it was determined was not reported) along with the water-content profiles from the STONE database to then determine the velocity field as the velocity is equal to the quotient of the infiltration rate and the water-content: $v = q/\theta$. Thus, if the ‘representative’ water-content profiles do not also reflect the average water-content over the same period, then the resulting velocity field may over- or underestimate the actual water velocity that occurred over that period. In other words, the water-content and infiltration rate need to be compatible with each other. Furthermore, this approach does not consider the effect temporal variation in water flow may have on transport. This may misrepresent the effect of adsorption to the AWI due to the dependence of A_{aw} on saturation and non-linear nature of K_{aw} . The effect of temporal resolution on transport when the adsorption process is (highly) non-linear can be seen in fig. 12 from Tiktak et al. (2003), which shows the average concentration of a compound in the top half meter in groundwater. From the graph it is apparent that temporal resolution greatly affects the breakthrough of the compound. Even though it is hard to say if the effect would be as pronounced for PFAS, it is not advised to use this simplified approach (i.e. that of Spijker et al.) to describing the hydrology of the system as it may deviate from the worst-case assumption.

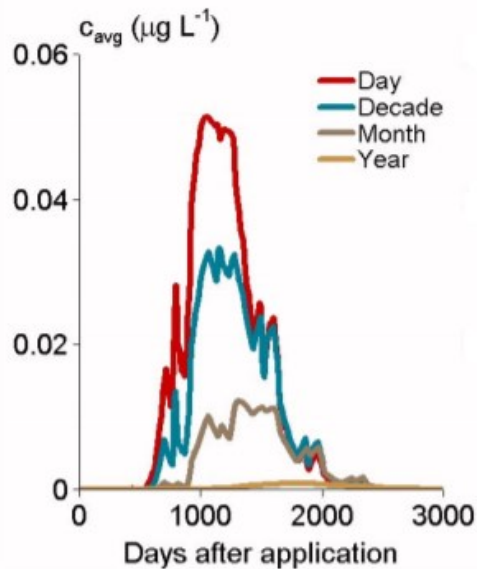


Figure 11 Graph illustrating the importance of a fine temporal resolution of the climatic data (i.e. infiltration). The scenario is of a compound leaching from the surface to the groundwater after having been applied on the surface (e.g. a pesticide), with the concentration (y-axis) representing the average concentration in the top 1m of the groundwater. It is assumed decade is supposed to mean 10 days. Image from Tiktak et al. (2003).

(86) The alternative approach is to define the soil-profile in terms of soil-hydraulic properties (e.g. Mualem-van Genuchten parameters) representative of the average Dutch soil, and then impose boundary conditions (i.e. climatic data and water-table depth) that are also representative of the average Dutch situation. The use of soil-hydraulic properties and boundary conditions is how models such as HYDRUS-1D and PEARL/SWAP determine flow in the unsaturated zone. Past climatic records can readily be obtained from the Royal Netherlands Meteorological Institute (KNMI). As for the other two aspects (i.e. the water-table depth and soil-hydraulic properties), other resources are available. The *Bodem(kundig) Informatie Systeem* (BIS; Bakker et al., 2017) contains Mualem-van Genuchten parameters for 132 samples collected throughout the Netherlands and at different depths, which could perhaps provide a means to derive an “average” Dutch soil-profile or set of soil-profiles. How this would be done exactly, however, is still uncertain. Alternatively, Verschoor et al. (2006) state that the PEARL model contains built-in soil profiles that are designed to represent the Dutch situation, and since PEARL relies on SWAP to describe the flow, which in turn used the Mualem-van Genuchten equations to solve the Richard’s equation for unsaturated flow, it stands to reason that representative Mualem-van Genuchten parameters are also available within PEARL. However, how these representative profiles were determined is still unclear. As for the depth to groundwater table, both Spijker et al. and Verschoor et al. assumed a groundwater table depth at 1m, which they say is a realistic worst-case scenario as in many places in the Netherlands the groundwater table is deeper than 1m. The benefit of using this approach, as opposed to the one used in Spijker et al., is that it allows for increased temporal resolution of the climatic conditions, which allows for a more realistic representation of reality. However, this approach would require further work to establish what a representative Dutch soil-profile would be in terms of soil-hydraulic properties and would likely require expert opinion. A source of inspiration could be the creators of the PEARL model (e.g. Dr. Aaldrik Tiktak), as they have apparently done a similar thing in the past.

4.2. Chemistry of the System

(87) When it comes to characterizing the chemistry of the system, in the context of partitioning (as opposed to a speciation model) this implies ascribing appropriate partitioning coefficients for adsorption to both solids and AWIs. Since the factors that control the partitioning coefficients (e.g.

OC, pH, ionic strength etc.) likely vary with depth, the partitioning coefficients (especially K_d) are also expected to vary with depth. As for how the factors that influence the partitioning coefficients vary in depth, the three 'typical' soil profiles reported in Spijker et al. (2009; from STONE database) can perhaps be used. This would, however, require a multiple regression analysis to account for the combined effect of the multiple factors on K_d . Furthermore, intuitively one may say there should be a link between the profile used to describe the chemistry of the system and the profile describing the hydrology. In other words, it would be questionable to use a profile with hydrological properties derived from the BIS database yet use the chemical properties from the STONE database. And since there does not appear to be any corresponding soil-hydrological properties for the STONE profiles used in Spijker et al., perhaps these profiles cannot be used. However, determining whether this would be a valid approach would require expert opinion. Alternatively, the standard Dutch profile reported in Tiktak et al. (2000) and used in Verschoor et al. (2006) could be used, as it was selected to represent a realistic worst-case scenario in terms of high leachability of pesticides applied to the surface. The profile data includes data on OM%, clay%, pH and other things, and as such could be used to determine how the partitioning coefficient K_d will vary in depth if a multiple regression analysis is done to account for the combined influence of all these factors. This further highlights the need for a multiple regression analysis. Nevertheless, should this worst-case scenario profile be based on the same soil profile as the built-in soil profile with soil-hydraulic properties within PEARL, then this would make it the two characterizations (i.e. hydrological and chemical) consistent with each other.

(88) Besides defining the chemistry of the soil profile, another important aspect are the initial conditions. Since the focus of the research is on leachability of PFAS from surface applied soil/sediment, similar initial conditions as in Spijker et al. (2006) are suggested due to the similarity of the context. The only difference is the compound(s) in question: here the interest is PFAS whereas there it was heavy metals. In Spijker et al. it is assumed that there is a 'natural' background level, which is found throughout the entire profile. The top 0.5m is then assumed to have elevated concentrations of the compounds in question (see fig. 13), which contains both this background level (*achtergrond*) and the anthropogenic addition (*aanrijking*). Both contributions consist of a fraction which is non-reactive since they are sorbed irreversibly to minerals. It is not sure to what degree this is the case for PFOA and PFOS (e.g. Milinovic et al., 2015), yet assuming completely reversible adsorption would be in line with the worst-case assumption. In Spijker et al. they assumed a total concentration in the top 0.5m equal to the *maximale waarde klasse wonen* (one of the soil criteria), and thus the *source term* (i.e. the leachable concentration in the top 0.5m) was equal to the *maximale waarde* minus the natural background concentration since the background concentration is found ubiquitously. A similar methodology might be applicable for modelling PFAS transport in the unsaturated zone in the context of evaluating/determining suitable criteria, yet this would need to be verified.

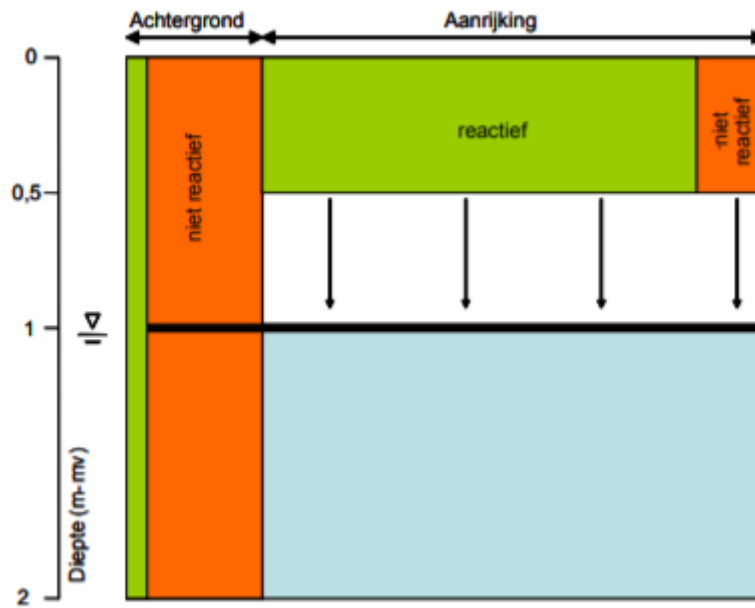


Figure 12 Image showing the design of the model setup used in Spijker et al. (2009). This study investigated the impact of heavy metals leaching from surface applied soil/sediment on the groundwater. The non-reactive fractions are due to metals being adsorbed irreversibly. The “aanrijking” + “achtergrond” combined equal the “maximale waarde”, with the source term being described as the “aanrijking” (i.e. “maximale waarde” – “aanrijking”). Image from Spijker et al. (2009).

5. Modelling Exercise

5.1. Approach

(89) The approach of the modelling exercise is based on the retardation factor, which comes from the ADE (eq. 21, chapter 3). The logic behind using the retardation factor is that it can give a first approximation of PFAS transport for a given system. If we assume that adsorption on both solids and AWI are instantaneous or relatively fast compared to the groundwater flow rate (i.e. described by equilibrium adsorption) and follow a linear isotherm (i.e. use of K_d), then these processes effectively retard transport of the solute and eq. 21 (chapter 3) can be rewritten in terms of a retardation factor:

$$(\theta \cdot R_f) \frac{\partial C}{\partial t} = -\theta \cdot v \cdot \frac{\partial C}{\partial z} + \frac{\partial}{\partial z} \left(\theta \cdot D \cdot \frac{\partial C}{\partial z} \right) \quad (22)$$

Where,

$$R_f = 1 + \frac{\rho_b \cdot K_d}{\theta} + \frac{A_{awi} \cdot K_{awi}}{\theta} \quad (23)$$

(90) is the retardation factor (e.g. Brusseau, 2018). Note that $\theta \cdot v$ in the advective term can only be taken out of the derivative under the condition of constant infiltration/flux (since $q = \theta \cdot v$). R_f can be brought to the other side of the equation to give:

$$\theta \frac{\partial C}{\partial t} = -\theta \cdot \frac{v}{R_f} \cdot \frac{\partial C}{\partial z} + \frac{1}{R_f} \cdot \frac{\partial}{\partial z} \left(\theta \cdot D \cdot \frac{\partial C}{\partial z} \right) \quad (24)$$

(91) Important to keep in mind is that the ADE is based on conservation of mass: change in mass (i.e. concentration) *in a given volume* has to be equal to the mass coming in minus the mass going out,

assuming no sources or sinks in the volume. This equation is intended for *local* changes in mass: changes in infinitesimally small volumes ($z \rightarrow z+\partial z$, where ∂z approaches 0), but the principle holds for a volume of any size. With this in mind, a way to interpret this new formulation is as follows: for a given interval (∂z , analogous to volume), which is characterized by a single water-content (and thus also specific interfacial area), the apparent velocity with which a solute travels over that interval is smaller than the actual pore-water velocity by a factor R_f . When it comes to numerical modelling, each interval, ∂z , is considered as a discrete interval, Δz . Generally, you would want to minimize these intervals to avoid spurious results due to discretization errors, at the cost of computation time. However, if you were able to obtain values for the properties/characteristics of a given interval that are representative of that interval (i.e. accounting for spatial heterogeneities in properties), then perhaps larger intervals can be considered. These representative values can be regarded as a type of average value of any given property for a given interval. The properties for which representative values need to be determined to calculate R_f are the two partitioning coefficients (K_d and K_{awi}), bulk density (ρ_b), water-content (θ), and specific air-water interfacial area (A_{awi}).

(92) To determine what the representative values of these properties are, it is easier to start with a simple scenario where there is a single soil type in a depth profile, implying that K_d is constant in depth. Looking at the left-hand side of eq. 21 (chapter 3), the terms from which R_f is ‘extracted’ (i.e. the time-dependent terms) describe the *total* change in mass in the *total* volume, and as such the values of ρ_b , θ , and A_{awi} are the *total* mass of solid, volume of water, and interfacial surface area, respectively, per unit of *total* volume. Following this logic, appropriate values for ρ_b , θ , and A_{awi} for a larger interval would also be the total of the respective units per unit of the total volume. For a given steady-state water-content profile this would equate to the space-averaged (i.e. depth-averaged) values of each parameter since they are all defined as per unit volume and in the case of a 1D domain space-averaging is the same as volume-averaging. The implication of this is that for any steady-state unsaturated flow, the retardation of a solute whose adsorption behaviour is linear and instantaneous, retardation can be estimated solely on the steady-state water content profile. This is an important finding because it circumvents needing modelling software that explicitly accounts for interfacial adsorption, since that software does not yet exist for public use (e.g. Guo et al., 2020), albeit the scope of use is limited in terms of scenarios that can be simulated. The following section will focus on the results of this approach: first a validation case will be shown and then the results of a sensitivity analysis.

5.2. Methods

5.2.1. Validation Case

(93) Initially a validation case will be tested. This validation case is supposed to validate the hypothesis that averaging the water-content in space over an interval provides a representative θ that can be used to determine the R_f over that interval. For the validation case, a solute that only undergoes solid-phase adsorption is considered, so the third term in the retardation factor expression (eq. 23, section 5.1.) is zero (i.e. no air-water interfacial adsorption). As discussed above, the adsorption process is described by linear and equilibrium adsorption ($K_d = 3$ L/kg). The scenario consists of a soil profile with steady-state flow resulting from constant infiltration from the top of the profile ($q=30$ cm/year), with the groundwater table found at 1m depth. The steady-state flow conditions were determined using HYDRUS-1D, with the soil-hydraulic parameters necessary for the Mualem-Van Genuchten equations based on a sandy-loam soil (parameter values are available in the HYDRUS-1D interface). The steady-state water-content profile is shown below, and an observation point is placed at 1m.

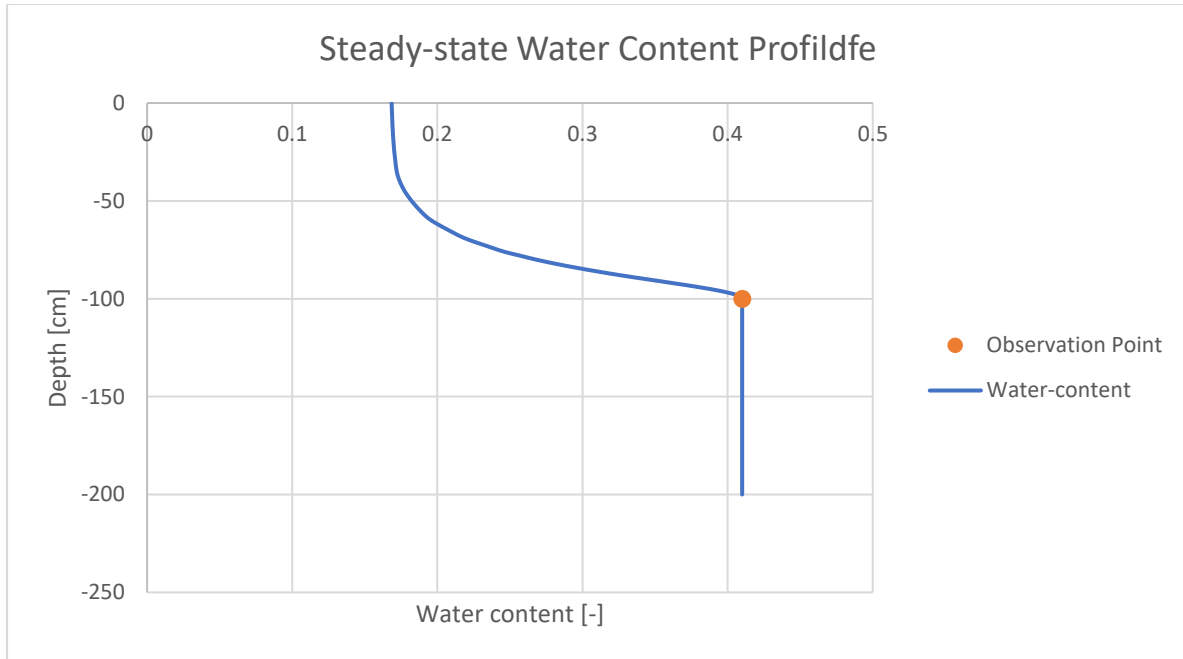


Figure 13 Steady-state water content profile for the case of constant infiltration: $q=-30\text{cm/yr}$.

(94) The observation point signifies the interval over which the retardation factor is determined (i.e. from 0-1m depth), and over that interval the average θ was found to be 22%. Given a K_d of 3 L/kg and ρ_b of 1.5 kg/L, and using eq. 23 (without the last term; section 5.1.) R_f can be calculated. This result is then compared to the ‘actual’ R_f as simulated with HYDRUS-1D; since the software is capable of simulating transport of both an NRT ($K_d=0$) and an adsorbing solute ($K_d=3$), the retardation factor for breakthrough at 1m can be determined by comparing the breakthrough curves. The actual R_f is determined by dividing the peak-concentration time of the adsorbing solute to the peak-concentration time of the NRT:

$$R_{f_actual} = \frac{t_{peak_adsorbing-solute}}{t_{peak_NRT}} \quad (25)$$

(95) The initial conditions with respect to initial concentration distribution is that the compounds (i.e. adsorbing solute and NRT) are found in the top 0.5m of the soil profile, with the same initial total mass.

5.2.2. Sensitivity Analysis

(96) For the sensitivity analysis, the sensitivity of R_f to the varying parameters is explored. Variations in infiltration rate, K_d , K_{awi} , and A_{max} (a parameter required to estimate A_{awi} as a function of saturation: $S_w=\theta/\varphi$, with φ being the porosity) are considered. There are several (empirical) expressions relating A_{awi} to saturation (section 2.3.1.), each requiring a different set of parameters. In this investigation the simplest relation is considered (e.g. Lyu et al., 2018; Kim et al., 1997), namely a linear expression. This relation was chosen because it requires the least amount of information (only 1 parameter). The representative PFAS is PFOS, and so variations in K_d and K_{awi} will reflect variations in reported values of these parameters in literature. The assumption of linear adsorption for the solid-phase (i.e. use of K_d) is motivated by the fact that a lot of isotherms for PFOS adsorption in the literature where the Freundlich isotherm was used had values for the Freundlich exponent (n) that could statistically be unity, implying linear adsorption (see also Tables 3 and 5). Similarly, the use of a constant K_{awi} is motivated by the fact that for concentrations below 0.1 mg/L, which is on the high-end for most PFOS concentrations found in the field (with exception of heavily contaminated areas such as former fire-

fighting training sites), K_{awi} is essentially constant (Brusseau, 2019). However, as stated in section 2.3.4. there is reason to question this claim.

(97) For the steady-state flow condition and the breakthrough curves shown, the setup with respect to initial and boundary conditions is the same as what was used in the validation case. Namely, a soil profile of 2m is considered, with the groundwater table being fixed at ~ 1 m depth. A constant infiltration rate is imposed at the top of the boundary, and two infiltration rates are considered: -30 cm/year and -1000 cm/year. The lower end of the spectrum is based on the net yearly infiltration rate in the Netherlands (Spijker et al., 2009), and the upper limit was chosen to reflect a noticeable increase in average water-content, and thus also a decrease in A_{awi} . For the breakthrough curves shown, the initial conditions of the PFOS concentration distribution are also the same as for the validation case: in the top 0.5m of the soil profile. The value of the initial concentration corresponds to the Dutch norm 'Maximale Waarden Klasse Wonen' (18 $\mu\text{g}/\text{kg}$; Wintersen et al., 2019), and is $\sim 3 \cdot 10^{-2}$ mg/L assuming a bulk density of 1.5 kg/L (**Note:** concentration here is not per litre of water but volume of soil: water+solid+air. It is calculated by multiplying the *Maximale Waarden Klasse Wonen* by the soil density).

Table 7 Base values used in the sensitivity analysis.

Property	Base Value
K_d [L/kg]	10
K_{awi} [cm]	0.1
A_{max} [cm^{-1}]	300
q [cm/yr]	-30
R_f [-]	129

(98) To carry out a sensitivity analysis, first a base scenario needs to be established in terms of base values of the different parameters. These values are summarized in the table above (table 7). The soil type considered, in terms of soil hydraulic properties, is a sandy-loam, with the values for the Mualem-van Genuchten parameters as defined in HYDRUS-1D. The base value for K_d is partially arbitrary, but it lies within the range of reported K_d values for PFOS. The value for K_{awi} is taken from Guo et al. (2020), yet this value is different to other reported values (e.g. Brusseau, 2019) and so these variations will also be considered in the sensitivity analysis. The choice of 300 cm^{-1} as the base value for A_{max} is also partially arbitrary: this parameter varies by several orders of magnitude in the literature and is dependent on the method used in its determination (see section 2.3.1.). Thus, this value was chosen to give reasonable retardation factors/breakthrough times yet is still within the range of values reported in the literature. The resulting predicted retardation factor for this system is 129, and the breakthrough curve is shown below (fig. 15). For reference, the peak concentration of the NRT at 1m depth occurred after ~ 0.6 months.

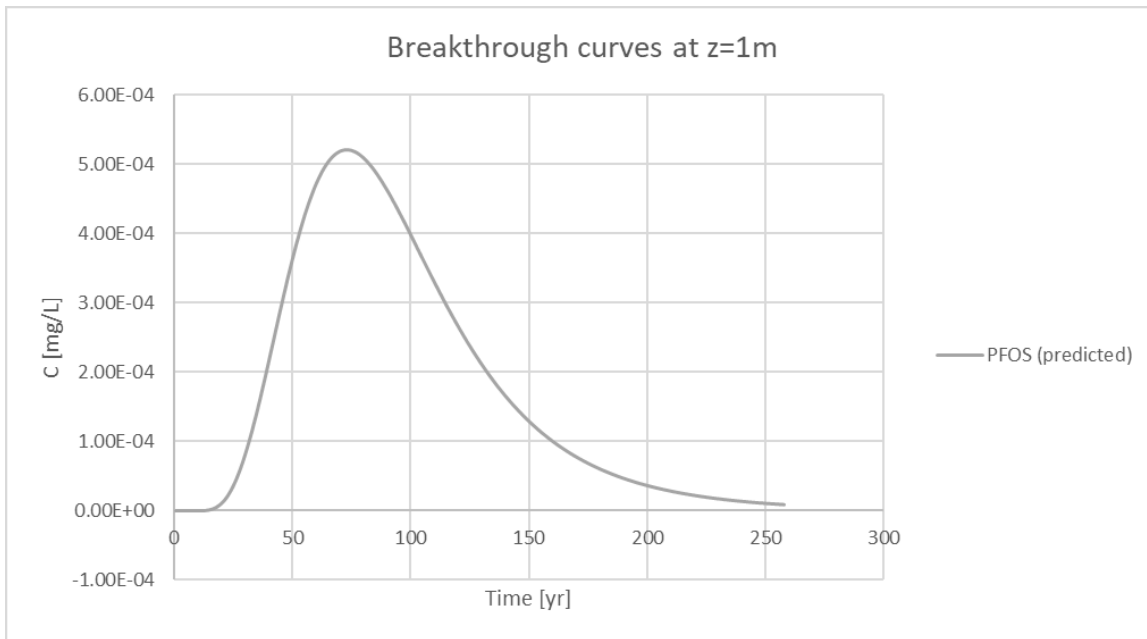


Figure 14 Breakthrough curve for the base-scenario (i.e. using base values listed in table 7).

5.3. Results

5.3.1. Validation Case

(99) The results of the validation case can be seen below (fig. 16). The peak-concentration time of the NRT was ~ 0.54 years, and for the adsorbing solute it was ~ 11.13 years, which gives an R_{f_actual} of 20.5. This result compares reasonably well with the approximation, which gave an R_f of 21.5. With the R_f of the approximation, a breakthrough curve at 1m can be reconstructed using the breakthrough data for the NRT by multiplying each time of the breakthrough curve for the NRT by the estimated R_f . The resulting breakthrough curve is shown below alongside the simulations done with HYDRUS-1D.

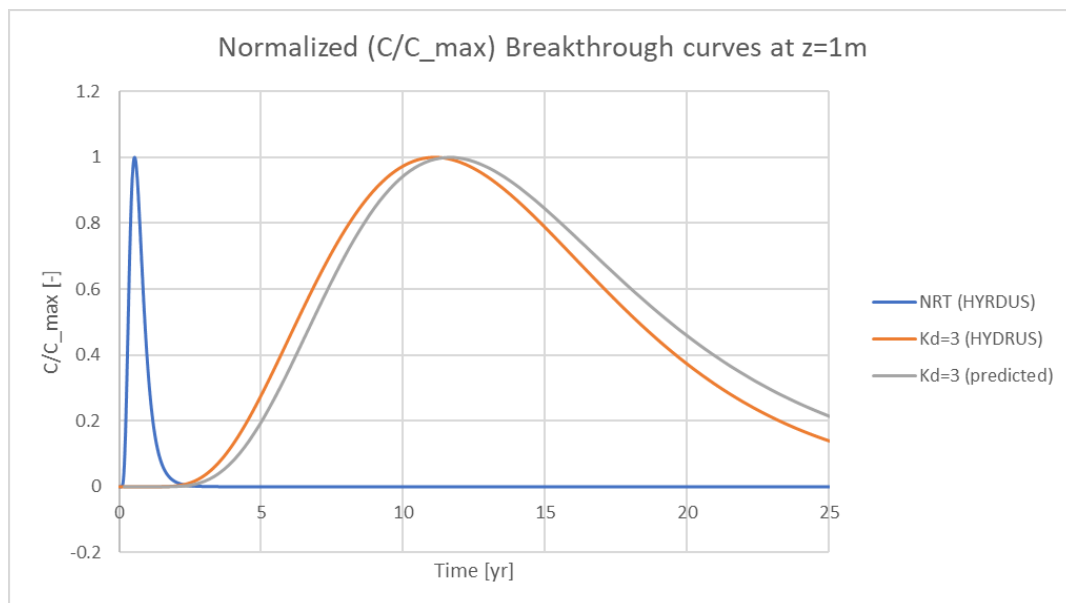


Figure 15 Graph showing the results of the validation case. Concentrations are normalized to the peak concentration to facilitate comparison. The blue line is the breakthrough for an NRT, the orange line for an adsorbing solute ($K_d=3$), and grey line as predicted using eq. 23 without the last term (i.e. $K_{dwi}=0$).

5.3.2. Sensitivity Analysis

(100) The results of the sensitivity analysis are shown here. The steady-state water-content profiles for the two tested infiltration rates can be seen in figures 17 and 18. Noticeable is the difference in the average water-content in the top part of the profiles: for an infiltration rate of 1000 cm/yr the water content in the top ~75 cm is around 0.28, whereas for the infiltration rate of 30 cm/yr the water content is less than 0.2. On average, the profile of the higher infiltration rate is more saturated, which is to be expected.

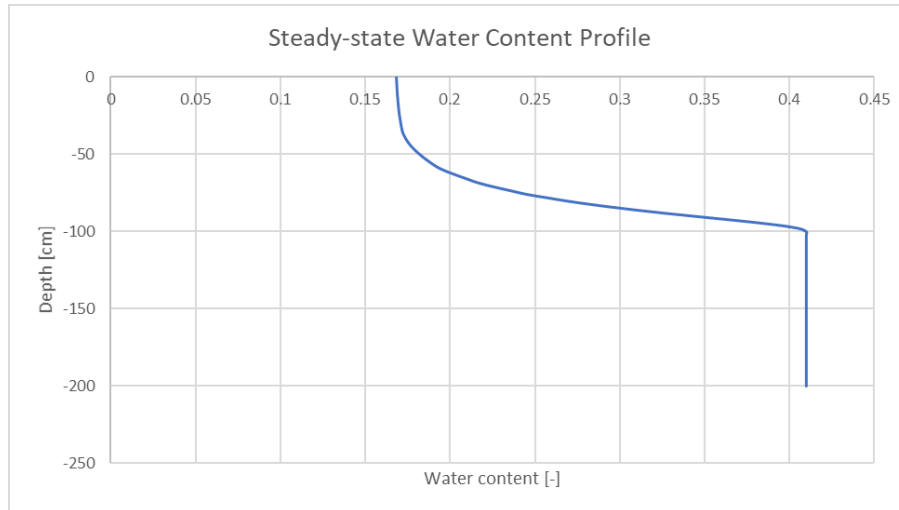


Figure 16 Steady-state water content profile for infiltration rate of 30 cm/yr.

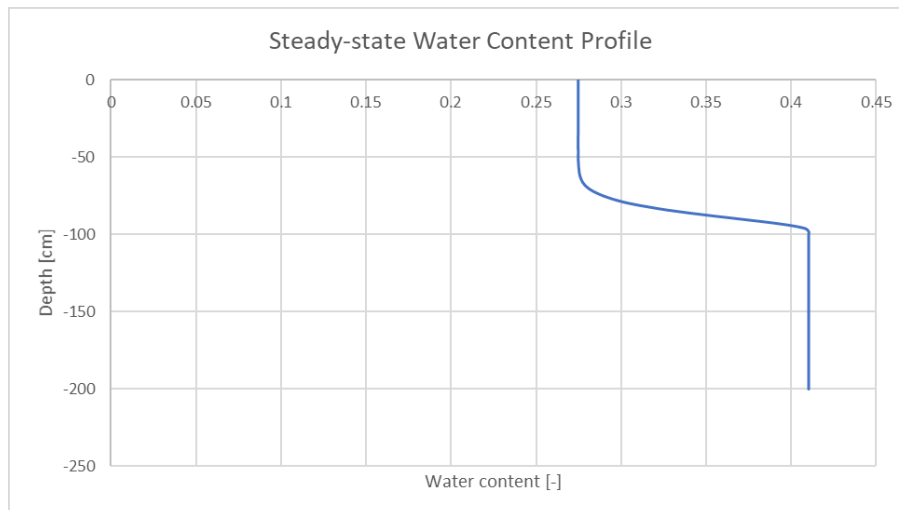


Figure 17 Steady-state water content profile for infiltration rate of 1000 cm/yr.

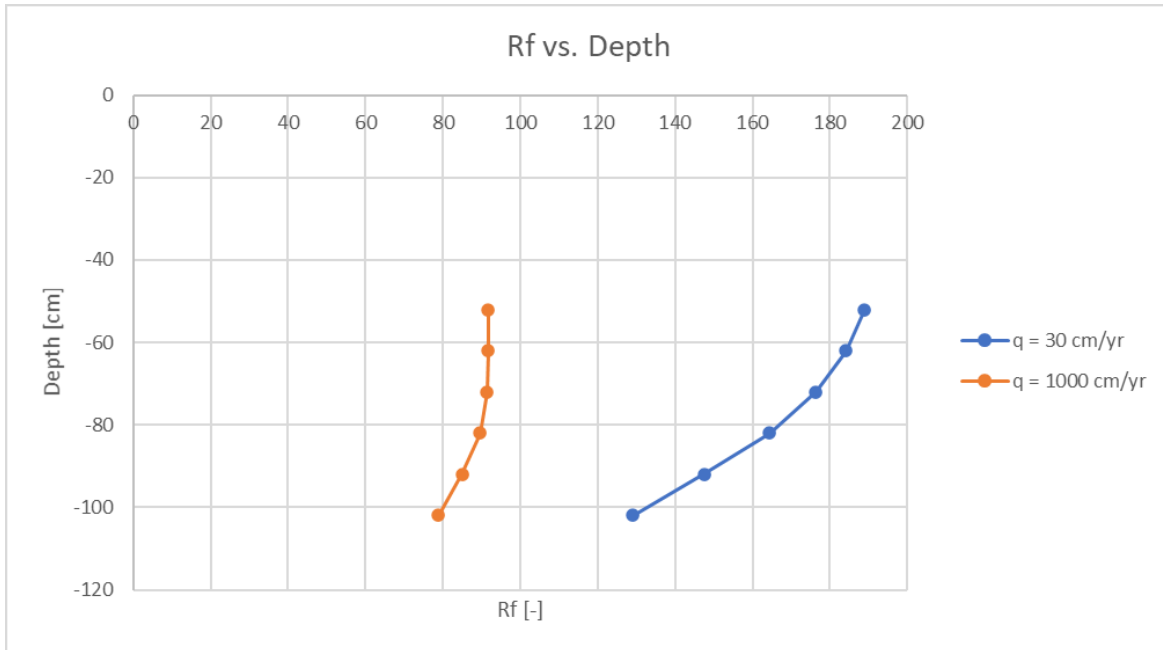


Figure 18 Plot of R_f vs. depth for base conditions at the two tested infiltration rates. Note: the R_f does not represent the retardation at that depth, but rather how much retardation occurs from $z=0$ till that depth.

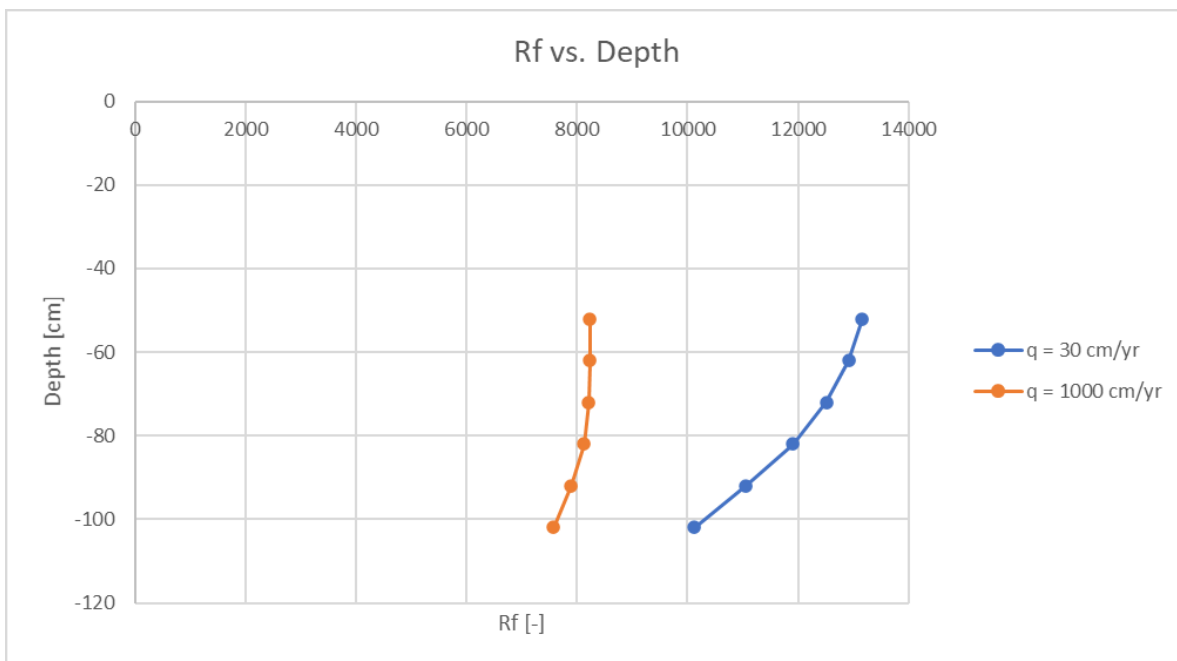


Figure 19 Plot of R_f vs. depth for $K_d=1500$ at the two tested infiltration rates. Note: the R_f does not represent the retardation at that depth, but rather how much retardation occurs from $z=0$ till that depth.

(101) Figures 19 and 20 show how the R_f changes with depth. Noticeable differences between the two tested infiltration rates can be seen in the shape of the curves. For the low infiltration rate the retardation factor decreases more with each unit in depth when compared to the high infiltration rate. This is likely due to the differences in the water-content profiles: for the low infiltration rate the water-content increases “faster” as the depth increases.

(102) The K_d 's considered in the sensitivity analysis are shown in table 8. The spread includes data from the literature, and also recent data from batch experiments done by the RIVM. The range in R_f is the greatest when compared to range of R_f for the other terms. Also, the effect of K_d on R_f appears to not be affected by the higher infiltration rate.

Table 8 Results for the sensitivity analysis when K_d is being changed and everything else kept at the base value.

K_d [L/kg]	R_f [-]		Peak Conc. [ug/L]		Comments/source
	30 cm/yr	1000 cm/yr	30 cm/yr	1000 cm/yr	
0.15	63	29	1.07	1.99	For sand medium; Brusseau et al. (2019a)
10	129	79	0.52	0.74	Base value
66	504	361	0.13	0.16	Lowest K_d from recent RIVM batch experiments
280	1940	1438	$3.47 \cdot 10^{-2}$	$4.04 \cdot 10^{-2}$	Median K_d from recent batch experiments
1500	~10000	7579	$6.64 \cdot 10^{-3}$	$7.67 \cdot 10^{-3}$	High-end K_d from recent batch experiments

(103) The reference values used for K_{awi} were taken from a variety of sources. It appears from the variations found in the literature the parameter does not appear to have as much of an effect when compared to K_d and A_{max} .

Table 9 Results for the sensitivity analysis when K_{awi} is being changed and everything else kept at the base value. The retardation factors and peak concentrations for the smallest K_{awi} are virtually the same for a K_{awi} of 0.

K_{awi} [cm]	R_f [-]		Peak Conc. [ug/L]		Comments/source
	30 cm/yr	1000 cm/yr	30 cm/yr	1000 cm/yr	
$2.3 \cdot 10^{-3}$	69	52	0.97	1.12	Surface tension data; from Brusseau (2019a)
0.02	80	57	0.84	1.02	From miscible-displacement experiments; from Brusseau et al. (2019a)
0.1	129	79	0.52	0.74	Base value; from Guo et al. (2020)
1	677	326	$9.92 \cdot 10^{-2}$	0.18	Approximate value at PFOS concentration of 500 ng/L; from Schaefer et al. (2019)

(104) As for the effect of A_{max} on retardation, it does not appear to have as much of an effect as K_d in terms of the range of the magnitude of the retardation factor. As expected, the range of values for R_f is even less under the higher infiltration than the lower infiltration.

Table 10 Results for the sensitivity analysis when A_{max} is being changed and everything else kept at the base value.

A_{max} [cm ⁻¹]	R_f [-]		Peak Conc. [ug/L]		Comments/source
	30 cm/yr	1000 cm/yr	30 cm/yr	1000 cm/yr	
65	81	57	0.83	1.01	For sand column estimated with linear expression; from Kim et al. (1997)
300	129	79	0.52	0.74	Base value
1000	271	143	0.25	0.41	Mid-range value

10000	2100	968	$3.20 \cdot 10^{-2}$	$6.00 \cdot 10^{-2}$	Within range reported in Peng & Brusseau (2005). Determined with gas-phase method (see section 2.3.1.)
-------	------	-----	----------------------	----------------------	--

5.4. Discussion + Conclusions

(105) The results of the validation case can be seen in fig. 16. Looking at the breakthrough curves the approximation does show slight deviation, indicated by the shift in the curves. However, the closeness of the two retardation factors would suggest that the proposed approach through averaging water-content in space is valid to estimate R_f over a given interval. The overestimation in R_f is attributed to the initial conditions and the nature of the approach. The predicted R_f assumes that *all* of solute will travel over the length over which R_f is determined, namely from 0-1m depth. However, the initial conditions have the solute initially present down to a depth of 0.5m, and thus not all of the solute travels through the entire length of 0 to -1m. If the initial conditions were such that the solute was only found in, for example, the top 5cm of the soil profile, it is expected that the predicted R_f will be much closer to the *actual* R_f . Nonetheless, since this method of averaging appears to be valid for θ , it is thus also expected to be valid for A_{awi} when considering air-water interfacial adsorption. However, this would need to be validated with either experiments or modelling software, neither of which are viable options for this research.

(106) With respect to the sensitivity analysis, several important observations are made. First is that the range of calculated R_f 's is quite large, ranging from 63-~10000 for the $q=30$ cm/yr and from 29-7579 for $q=1000$ cm/yr. Similarly, the peak concentration also varies several orders of magnitude, between $\sim 7 \cdot 10^{-3}$ -2 ug/L. Considering all the values selected for the sensitivity analysis are based on actual values from the literature that could potentially apply to the Dutch situation, it indicates that the amount of retardation can vary significantly geographically. In other words, this means that the mobility of PFAS could vary a lot in the Netherlands. Of course, this depends on the whether the analyzed factors vary to the same degree in Dutch soils, but it does give more credence to assuming a worst-case scenario. Another important finding is the apparent hierarchy regarding the sensitivity of R_f to the factors. K_d appears to have the greatest impact on R_f , followed by A_{max} and then K_{awi} . This is not determined by comparing the amount of incremental change in R_f per incremental change of a parameter, but rather based on the spread of R_f values. The large spread in R_f for varying K_d is due to the large spread in K_d values. This highlights how the fickle nature of K_d can greatly impact transport. Simultaneously, the comparatively small spread in R_f for changing K_{awi} is due to the low values for K_{awi} . The small values for K_{awi} also impact the sensitivity of R_f to A_{max} since K_{awi} and A_{awi} (and thus A_{max}) are multiplied by each other. Thus the sensitivity of R_f to these terms is also dependent on the magnitude of both parameters together.

(107) Regarding the effect of infiltration rate, a higher infiltration rate invariably reduces the R_f , which is expected when looking at eq. 23 (section 5.1). As for the change in R_f with depth for the two infiltration rates, as expected R_f shows greater variability in depth for the slow infiltration rate than the fast rate. This is to be expected by looking at the water-content profiles: the water-content profile for the low infiltration rate exhibits a much greater change over the depth. This not only affects the R_f directly, but also indirectly by affecting A_{awi} . However, the implications of this for the Dutch situation are not clear. It does, however, lead to questioning the effect of transient flow conditions, which is a better representation of reality. During transient flow conditions, the water-content profiles will change in time, and as such the retardation factor in depth will also vary in time. It is not clear what kind of effect this would have but it is worth investigating. A glimpse of what may be the case can be seen in figure 12 (section 4.1.). That graph showed the effect of temporal resolution of climate data

(i.e. infiltration), with the results being that using a coarse resolution would drastically underestimate transport and thus the peak concentration. A coarse temporal resolution is somewhat analogous to assuming steady-state conditions since if the temporal resolution is so coarse, enough time will pass such that steady-state will be achieved. Inversely, a fine temporal resolution with respect to infiltration rate would be equivalent to assuming transient conditions. Further investigation should also entail the effect of temporal resolution of infiltration rate since assuming steady-state conditions might deviate from the worst-case assumption.

(108) With respect to the concept of the worst-case assumption, within the current modelling framework (i.e. as described in section 5.1) choices can be made to get closer to the realistic worst-case scenario. These choices would be selecting the lowest realistic values for K_d , K_{awi} , and A_{max} , such that retardation in the unsaturated zone is minimal and the peak concentration is maximal. An unrealistic worst-case scenario would be to say $K_{awi}=K_d=0$, yet this would not be realistic since PFOA and PFOS have positive values for these two parameters. Nevertheless, if under these conditions the groundwater criteria are met, then that would mean that the groundwater is likely protected under most circumstances since it is protected under this unrealistic “worst-case”. However, if under this assumption it appears that the soil criteria are too low then this may have undesirable consequences. In such a case, it may be sensible to redefine the scenario such that it is still conservative, and in that sense still a sort of worst-case scenario, but more realistic than the original worst-case scenario. From that perspective, having the ability to model more processes provides flexibility and freedom in choosing a worst-case scenario since there are more possibilities.

(109) To conclude the modelling exercise, the approach has shown to be able to account for adsorption to both solid surfaces and AWIs, along with the transport processes. This allows to simulate transport of PFOA and PFOS in the unsaturated zone while accounting for all relevant processes, even though no public software exists yet to model such systems. From the sensitivity analysis, adsorption to solid surfaces (i.e. K_d) is responsible for the most variation in retardation, which is due to the wide range in K_d values. K_{awi} is responsible for the least variation in retardation, which is due to the low values of K_{awi} . While this approach is able model all relevant processes (i.e. transport, adsorption to solids, and adsorption to AWIs), there are still some aspects which cannot be taken to account. One such aspect is transient flow conditions, which is expected to be important in describing a realistic worst-case scenario. Other aspects which were not discussed is the influence of a heterogeneous soil-profile in terms of partitioning behaviour (i.e. K_d). The influence of these aspects is not yet known, and as such not knowing them could inadvertently mean a deviation from the worst-case scenario. More robust software is necessary to evaluate these questions. In appendix I, newly acquired software capable of evaluating the effect of transient flow conditions will be discussed and its capabilities reviewed.

6. Summary + Final Remarks

(110) In summary, this report details the different aspects that need to be considered when wanting to model vertical transport of PFOA and PFOS in the unsaturated zone, and specifically for the Dutch situation. In Chapter 1, the situation surrounding PFAS (especially PFOA and PFOS) was briefly discussed, and particularly in the context of the Netherlands. Namely, the need for modelling vertical transport of PFAS (especially PFOA and PFOS) in the unsaturated zone comes from the need to determine and/or evaluate suitable PFAS soil criteria (i.e. concentration norms for application of soil/sediment at another site).

(111) Chapter 2 described the 3 most important processes controlling fate and transport of surfactant PFAS (e.g. PFOA & PFOS) in the unsaturated zone, as determined from the literature, which are: transport processes (i.e. advection, dispersion, & diffusion), adsorption to solid surfaces, and adsorption to air-water interfaces. These processes were discussed in terms of the factors that control and influence them, and where possible a quantification of the influence of these factors was given. The idea behind quantifying the relation between the factors and the processes is so that a scenario can be established in which these factors are present, and thus the influence of these factors on the key processes would then be able to be quantified. From this chapter, the most important finding is that the solid-phase adsorption coefficient (K_d) appears to be dependent on numerous factors and there is no way (as of yet) to quantify the combined effect of these processes on K_d . The usual way of describing partitioning for organic compounds is to use the OC normalized K_d , K_{OC} , yet from the literature it appears on this cannot be used reliably for either PFOA or PFOS. Alternative approaches must be determined, either through assembling data from the literature to carry out a multivariate regression analysis, or some other means. Alternatively, under assumption of the worst-case, a selection of (low) partitioning coefficients could be selected from the literature. However, how this selection procedure would occur, especially with keeping in mind that the average Dutch situation is sought after, is unknown.

(112) In chapter 3 the knowledge from chapter 2, along with the literature, was used to establish a governing equation that is appropriate for modelling PFOA and PFOS in the unsaturated zone. This equation (eq. 20) takes into account the transport processes, adsorption to solids, and also adsorption to AWIs. Eq. 20, and to some extent eq. 21 (under certain assumptions), can be used as a blueprint to either create a reactive transport model, or to validate the use of other models/software. Until recently there was no available model capable of modelling reactive transport in the unsaturated zone while accounting for adsorption to the AWI. This software, which is a modified version of HYDRUS-1D, will be elaborated on in the Appendix. Like with the model shown in Guo et al. (2020), the governing equation is practically identical to eq. 20, the only difference that it includes more terms to account for other processes.

(113) Chapter 4 focused on the characterization of scenarios in the context of protecting the groundwater in the Netherlands from PFAS leaching from the surface. As such, the concept of the “average Dutch situation” was introduced. The average Dutch situation/scenario implies that any results from a modelling exercise can be deemed as representative for the average Dutch situation. This concept should be applicable to the description of both the hydrological and chemical system of the scenario. Different approaches to describing both the hydrological and chemical system were discussed, along with the benefits and limitations. For the hydrological model it was advised to use a more mechanistic model like PEARL or HYDRUS-1D due to the ability to account for transient conditions with respect to the climatic data (i.e. infiltration). Based on the simulations shown in Tiktak et al. (2003; fig. 12 in section 4.1) it is expected that not accounting for transient conditions may inadvertently deviate from the worst-case assumption.

(114) Finally, in chapter 5 the approach and results of a modelling exercise were discussed. The approach relies on special treatment of eq. 21 under the assumption of steady-state infiltration, and thus allows use of the retardation factor. The approach was (semi) validated, and was used to conduct a sensitivity analysis of several parameters that have direct influence on the retardation factor and thus transport. The values of the parameters used in the sensitivity analysis were nearly all retrieved from the literature and could hypothetically be representative for a Dutch situation. Considering this, the most astonishing result is the wide range in retardation factors that were predicted, indicating that mobility of PFAS (in this case PFOS) could be significantly variable from location to location. This

further emphasizes the importance of assuming a realistic worst-case to ensure that transport of surfactant PFAS to the groundwater is indeed limited by the imposed soil criteria.

References

- Ahrens, L., Taniyasu, S., Yeung, L., Yamashita, N., Lam, P., & Ebinghaus, R. (2010). Distribution of polyfluoroalkyl compounds in water, suspended particulate matter and sediment from Tokyo Bay, Japan. *Chemosphere*, 79(3), 266-272. <https://doi.org/10.1016/j.chemosphere.2010.01.045>
- Ahrens, L., Yeung, L., Taniyasu, S., Lam, P., & Yamashita, N. (2011). Partitioning of perfluorooctanoate (PFOA), perfluorooctane sulfonate (PFOS) and perfluorooctane sulfonamide (PFOSA) between water and sediment. *Chemosphere*, 85(5), 731-737. <https://doi.org/10.1016/j.chemosphere.2011.06.046>
- Bakker, G., Heinen, M., de Groot, W., Assinck, F., Hummelink, E., & Wesseling, J. (2017). Bodemhydrofysische gegevens in BRO en BIS : update 2016. Retrieved from <https://edepot.wur.nl/408308>
- Becker, A., Gerstmann, S., & Frank, H. (2008). Perfluorooctanoic acid and perfluorooctane sulfonate in the sediment of the Roter Main river, Bayreuth, Germany. *Environmental Pollution*, 156(3), 818-820. doi: 10.1016/j.envpol.2008.05.024
- Bradford, S., & Leij, F. (1997). Estimating interfacial areas for multi-fluid soil systems. *Journal Of Contaminant Hydrology*, 27(1-2), 83-105. doi: 10.1016/s0169-7722(96)00048-4
- Brusseau, M. (2018). Assessing the potential contributions of additional retention processes to PFAS retardation in the subsurface. *Science Of The Total Environment*, 613-614, 176-185. <https://doi.org/10.1016/j.scitotenv.2017.09.065>
- Brusseau, M. (2019). The influence of molecular structure on the adsorption of PFAS to fluid-fluid interfaces: Using QSPR to predict interfacial adsorption coefficients. *Water Research*, 152, 148-158. doi: 10.1016/j.watres.2018.12.057
- Brusseau, M., Khan, N., Wang, Y., Yan, N., Van Glubt, S., & Carroll, K. (2019a). Nonideal Transport and Extended Elution Tailing of PFOS in Soil. *Environmental Science & Technology*, 53(18), 10654-10664. doi: 10.1021/acs.est.9b02343
- Brusseau, M., El Ouni, A., Araujo, J., & Zhong, H. (2015). Novel methods for measuring air–water interfacial area in unsaturated porous media. *Chemosphere*, 127, 208-213. doi: 10.1016/j.chemosphere.2015.01.029
- Brusseau, M., Peng, S., Schnaar, G., & Costanza-Robinson, M. (2006). Relationships among air-water interfacial area, capillary pressure, and water saturation for a sandy porous medium. *Water Resources Research*, 42(3). doi: 10.1029/2005wr004058
- Brusseau, M., Yan, N., Van Glubt, S., Wang, Y., Chen, W., & Lyu, Y. et al. (2019b). Comprehensive retention model for PFAS transport in subsurface systems. *Water Research*, 148, 41-50. <https://doi.org/10.1016/j.watres.2018.10.035>
- Burns, D., Ellis, D., Li, H., McMurdo, C., & Webster, E. (2008). Experimental pKa Determination for Perfluorooctanoic Acid (PFOA) and the Potential Impact of pKaConcentration Dependence on Laboratory-Measured Partitioning Phenomena and Environmental Modeling. *Environmental Science & Technology*, 42(24), 9283-9288. doi: 10.1021/es802047v
- Cary, J. (1994). Estimating the surface area of fluid phase interfaces in porous media. *Journal Of Contaminant Hydrology*, 15(4), 243-248. doi: 10.1016/0169-7722(94)90029-9
- Chen, H., Zhang, C., Yu, Y., & Han, J. (2012). Sorption of perfluorooctane sulfonate (PFOS) on marine sediments. *Marine Pollution Bulletin*, 64(5), 902-906. doi: 10.1016/j.marpolbul.2012.03.012
- Chen, X., Zhu, L., Pan, X., Fang, S., Zhang, Y., & Yang, L. (2015). Isomeric specific partitioning behaviors of perfluoroalkyl substances in water dissolved phase, suspended particulate matters and sediments in Liao River Basin and Taihu Lake, China. *Water Research*, 80, 235-244. <https://doi.org/10.1016/j.watres.2015.04.032>
- CRC CARE. (2017). Assessment, management and remediation guidance for perfluorooctanesulfonate (PFOS) and perfluorooctanoic acid (PFOA) – Part 1: background, CRC CARE Technical Report no. 38.

- Costanza, J., Arshadi, M., Abriola, L., & Pennell, K. (2019). Accumulation of PFOA and PFOS at the Air–Water Interface. *Environmental Science & Technology Letters*, 6(8), 487-491. doi: 10.1021/acs.estlett.9b00355
- Costanza, M., & Brusseau, M. (2000). Contaminant Vapor Adsorption at the Gas–Water Interface in Soils. *Environmental Science & Technology*, 34(1), 1-11. doi: 10.1021/es9904585
- Costanza-Robinson, M., & Brusseau, M. (2002). Air-water interfacial areas in unsaturated soils: Evaluation of interfacial domains. *Water Resources Research*, 38(10), 13-1-13-17. doi: 10.1029/2001wr000738
- Ding, G., & Peijnenburg, W. (2013). Physicochemical Properties and Aquatic Toxicity of Poly- and Perfluorinated Compounds. *Critical Reviews In Environmental Science And Technology*, 43(6), 598-678. doi: 10.1080/10643389.2011.627016
- Du, Z., Deng, S., Bei, Y., Huang, Q., Wang, B., Huang, J., & Yu, G. (2014). Adsorption behavior and mechanism of perfluorinated compounds on various adsorbents—A review. *Journal Of Hazardous Materials*, 274, 443- 454. <https://doi.org/10.1016/j.jhazmat.2014.04.038>
- EPA. (1999). Understanding variation in partition coefficient, K_d values, *Volume I: The K_d Model, Methods of Measurement, and Application of Chemical Reaction Codes*.
- EPA. (2002). Hazard assessment of perfluorooctanoic acid and its salts.
- Enevoldsen, R., & Juhler, R. (2010). Perfluorinated compounds (PFCs) in groundwater and aqueous soil extracts: using inline SPE-LC-MS/MS for screening and sorption characterisation of perfluorooctane sulphonate and related compounds. *Analytical And Bioanalytical Chemistry*, 398(3), 1161-1172. <https://doi.org/10.1007/s00216-010-4066-0>
- Ferrey, M., Wilson, J., Adair, C., Su, C., Fine, D., Liu, X., & Washington, J. (2012). Behavior and Fate of PFOA and PFOS in Sandy Aquifer Sediment. *Groundwater Monitoring & Remediation*, 32(4), 63-71. <https://doi.org/10.1111/j.1745-6592.2012.01395.x>
- Guelfo, J., & Higgins, C. (2013). Subsurface Transport Potential of Perfluoroalkyl Acids at Aqueous Film-Forming Foam (AFFF)-Impacted Sites. *Environmental Science & Technology*, 47(9), 4164-4171. <https://doi.org/10.1021/es3048043>
- Guo, B., Zeng, J., & Brusseau, M. (2020). A Mathematical Model for the Release, Transport, and Retention of Per- and Polyfluoroalkyl Substances (PFAS) in the Vadose Zone. *Water Resources Research*, 56(2). doi: 10.1029/2019wr026667
- Henry, E., & Smith, J. (2003). Surfactant-Induced Flow Phenomena in the Vadose Zone: A Review of Data and Numerical Modeling. *Vadose Zone Journal*, 2(2), 154-167. doi: 10.2136/vzj2003.1540
- Higgins, C., & Luthy, R. (2006). Sorption of Perfluorinated Surfactants on Sediments†. *Environmental Science & Technology*, 40(23), 7251-7256. <https://doi.org/10.1021/es061000n>
- Johnson, R., Anschutz, A., Smolen, J., Simcik, M., & Penn, R. (2007). The Adsorption of Perfluorooctane Sulfonate onto Sand, Clay, and Iron Oxide Surfaces. *Journal Of Chemical & Engineering Data*, 52(4), 1165- 1170. <https://doi.org/10.1021/je060285g>
- Karkare, M., & Fort, T. (1996). Determination of the Air–Water Interfacial Area in Wet “Unsaturated” Porous Media. *Langmuir*, 12(8), 2041-2044. doi: 10.1021/la950821v
- Kim, H., Rao, P., & Annable, M. (1997). Determination of effective air-water interfacial area in partially saturated porous media using surfactant adsorption. *Water Resources Research*, 33(12), 2705-2711. doi: 10.1029/97wr02227
- Kim, H., Rao, P., & Annable, M. (1999). Gaseous Tracer Technique for Estimating Air-Water Interfacial Areas and Interface Mobility. *Soil Science Society Of America Journal*, 63(6), 1554-1560. doi: 10.2136/sssaj1999.6361554x
- Kwadijk, C., Korytár, P., & Koelmans, A. (2010). Distribution of Perfluorinated Compounds in Aquatic Systems in The Netherlands. *Environmental Science & Technology*, 44(10), 3746-3751. <https://doi.org/10.1021/es100485e>
- Li, Y., Oliver, D., & Kookana, R. (2018). A critical analysis of published data to discern the role of soil and sediment properties in determining sorption of per and polyfluoroalkyl substances (PFASs). *Science Of The Total Environment*, 628-629, 110-120. <https://doi.org/10.1016/j.scitotenv.2018.01.167>
- Lyu, Y., Brusseau, M., Chen, W., Yan, N., Fu, X., & Lin, X. (2018). Adsorption of PFOA at the Air–Water Interface during Transport in Unsaturated Porous Media. *Environmental Science & Technology*, 52(14), 7745-7753. doi: 10.1021/acs.est.8b02348

- Lyu, Y., & Brusseau, M. (2020). The influence of solution chemistry on air-water interfacial adsorption and transport of PFOA in unsaturated porous media. *Science Of The Total Environment*, 713, 136744. <https://doi.org/10.1016/j.scitotenv.2020.136744>
- Miao, Y., Guo, X., Dan Peng, Fan, T., & Yang, C. (2017). Rates and equilibria of perfluorooctanoate (PFOA) sorption on soils from different regions of China. *Ecotoxicology And Environmental Safety*, 139, 102-108. <https://doi.org/10.1016/j.ecoenv.2017.01.022>
- Milinic, J., Lacorte, S., Vidal, M., & Rigol, A. (2015). Sorption behaviour of perfluoroalkyl substances in soils. *Science Of The Total Environment*, 511, 63-71. doi: 10.1016/j.scitotenv.2014.12.017
- Ministerie van VROM. (2006). *NOBO: Normstelling en bodemkwaliteitsbeoordeling: Onderbouwing en beleidsmatige keuzes voor de bodemnormen in 2005, 2006 en 2007*. Den Haag.
- OECD. (2002). Hazard assessment of perfluorooctane sulfonate (PFOS) and its salts. Retrieved from <https://www.oecd.org/env/ehs/risk-assessment/2382880.pdf>
- Pan, G., Jia, C., Zhao, D., You, C., Chen, H., & Jiang, G. (2009). Effect of cationic and anionic surfactants on the sorption and desorption of perfluorooctane sulfonate (PFOS) on natural sediments. *Environmental Pollution*, 157(1), 325-330. <https://doi.org/10.1016/j.envpol.2008.06.035>
- Peng, S., & Brusseau, M. (2005). Impact of soil texture on air-water interfacial areas in unsaturated sandy porous media. *Water Resources Research*, 41(3). doi: 10.1029/2004wr003233
- Pereira, H., Ullberg, M., Kleja, D., Gustafsson, J., & Ahrens, L. (2018). Sorption of perfluoroalkyl substances (PFASs) to an organic soil horizon – Effect of cation composition and pH. *Chemosphere*, 207, 183-191. doi: 10.1016/j.chemosphere.2018.05.012
- Schaefer, C., Culina, V., Nguyen, D., & Field, J. (2019). Uptake of Poly- and Perfluoroalkyl Substances at the Air–Water Interface. *Environmental Science & Technology*, 53(21), 12442-12448. doi: 10.1021/acs.est.9b04008
- Schaefer, C., DiCarlo, D., & Blunt, M. (2000). Experimental measurement of air-water interfacial area during gravity drainage and secondary imbibition in porous media. *Water Resources Research*, 36(4), 885-890. doi: 10.1029/2000wr900007
- Schwarzenbach, R., Gschwend, P. and Imboden, D., 2003. *Environmental Organic Chemistry*. 2nd ed. New Jersey: John Wiley & Sons Inc.
- Smith, J., Beuthe, B., Dunk, M., Demeure, S., Carmona, J. M. M., Medve, A., . . . Slenders, H. (2016). Environmental fate and effects of polyand perfluoroalkyl substances (PFAS). 1-107.
- Spijker, J., Comans, R., Dijkstra, v., Groenenberg, B., & Verschoor, A. (2009). Uitloging van grond. Een modelmatige verkenning.
- Tiktak, A., van den Berg, F., Boesten, J., van Kraalingen, D., Leistra, M. and van der Linden, A., 2000. *Manual Of FOCUS PEARL Version 1.1.1*. De Bilt: RIVM, p.115.
- Tiktak, A., van der Linden, T., & Jjti, B. (2003). The GeoPEARL model. Description, applications and manual.
- Verschoor, A., Lijzen, J., van den Broek, H., Cleven, R., Comans, R., Dijkstra, J., & Vermij, P. (2006). Kritische emissiewaarden voor bouwstoffen Milieuhygiënische onderbouwing en consequenties voor bouwmaterialen.
- Vierke, L., Möller, A., & Klitzke, S. (2014). Transport of perfluoroalkyl acids in a water-saturated sediment column investigated under near-natural conditions. *Environmental Pollution*, 186, 7-13. <https://doi.org/10.1016/j.envpol.2013.11.011>
- de Voogt, P. (2010). Reviews of Environmental Contamination and Toxicology Volume 208. *Reviews Of Environmental Contamination And Toxicology*. doi: 10.1007/978-1-4419-6880-7
- Wintersen, A., & Otte, P. (2019). Overzicht van risicogrenzen voor PFOS, PFOA en GenX ten behoeve van een tijdelijk handelingskader voor het toepassen van grond en baggerspecie op of in de landbodem.
- Wintersen, A., Spijker, J., van Breemen, P., & van Wijnen, H. (2020). Achtergrondwaarden perfluoroalkylstoffen (PFAS) in de Nederlandse landbodem. doi: 10.21945/RIVM-2020-0100
- Wintersen, A., Oste, L., van der Meiracker, R., van Breemen, P. and Spijker, J., 2020. *Vershil In Uitloging Van PFAS Uit Grond En Bagger*. [online] RIVM. Available at: <https://www.rivm.nl/bibliotheek/rapporten/2020-0102.pdf> [Accessed 26 August 2020].
- Xiao, F., Simcik, M., Halbach, T., & Gulliver, J. (2015). Perfluorooctane sulfonate (PFOS) and perfluorooctanoate

- (PFOA) in soils and groundwater of a U.S. metropolitan area: Migration and implications for human exposure. *Water Research*, 72, 64-74. <https://doi.org/10.1016/j.watres.2014.09.052>
- You, C., Jia, C., & Pan, G. (2010). Effect of salinity and sediment characteristics on the sorption and desorption of perfluorooctane sulfonate at sediment-water interface. *Environmental Pollution*, 158(5), 1343-1347. <https://doi.org/10.1016/j.envpol.2010.01.009>
- Young, C., Furdui, V., Franklin, J., Koerner, R., Muir, D., & Mabury, S. (2007). Perfluorinated Acids in Arctic Snow: New Evidence for Atmospheric Formation. *Environmental Science & Technology*, 41(10), 3455-3461. doi: 10.1021/es0626234
- Zareitalabad, P., Siemens, J., Hamer, M., & Amelung, W. (2013). Perfluorooctanoic acid (PFOA) and perfluorooctanesulfonic acid (PFOS) in surface waters, sediments, soils and wastewater – A review on concentrations and distribution coefficients. *Chemosphere*, 91(6), 725-732. <https://doi.org/10.1016/j.chemosphere.2013.02.024>
- Zhi, Y. and Liu, J., 2018. Sorption and desorption of anionic, cationic and zwitterionic polyfluoroalkyl substances by soil organic matter and pyrogenic carbonaceous materials. *Chemical Engineering Journal*, 346, pp.682-691.

Appendix I : Modified HYDRUS-1D Model

The HYDRUS-1D model for saturated flow and reactive transport modelling has recently been modified by Prof. Dr. J. Simunek (HYDRUS creator and administrator) and his colleagues, and now facilitates modelling reactive transport of surfactant PFAS like PFOA and PFOS. The changes are similar to the suggested changes from some months prior, namely to replace the term describing concentration in the gas phase by concentration on the AWI (note the notation differs to the notation used throughout the rest of the report):

$$\frac{\partial \alpha_v \cdot g}{\partial t} = \frac{\partial \Gamma A_{aw}}{\partial t} \quad (A1)$$

Where α_v is the air content [$L^3 L^{-3}$], g is the concentration of a solute in the gas phase [$M L^{-3}$], Γ is the surface excess (i.e. same as C_{awi} in eq. 9) [$M L^{-2}$], and A_{aw} is the specific air-water interfacial area [$L^2 L^{-3}$]. Substitution of the right-hand-side in eq. A1 into the solute transport governing equation of HYDRUS gives an equation which is virtually identical to eq. 20, except that the equation in Hydrus includes several more terms to describe 1st and 0 order rates (i.e. source/sink terms). Also, instead of using an empirical relationship to calculate A_{aw} a relationship based on the theoretical approach by Bradford & Leij, 1997] is used:

$$A_{aw}(\theta) = \frac{1}{\sigma_{aw}} \int_{\theta}^{\theta_s} P_{aw}(\theta) d\theta = \frac{\rho_w g}{\sigma_{aw}} \int_{\theta}^{\theta_s} h(\theta) d\theta \quad (A2)$$

Where σ_{aw} is the air-water interfacial tension [$M T^{-2}$], P_{aw} is the capillary pressure [$M L^{-1} T^{-2}$], θ_s is the saturated water-content [$L^3 L^{-3}$], ρ_w is the density of water [$M L^{-3}$], and g is the acceleration due to gravity [$L T^{-2}$]. The specifics of how eq. A2 was derived was honestly too difficult to follow, but it does give values for A_{awi} which are of similar magnitude to the interfacial areas determined by the aqueous-phase interfacial tracer methods, and so can also be considered a *worst-case* since these values will still be smaller compared to the gas-phase methods (see section 2.3.1.).

The final modification is the description of Γ as a function of C (i.e. the isotherm). The modified Hydrus assumes that adsorption to the AWI is described by the Langmuir isotherm (i.e. eq. 17, section 2.3.2.). This too adheres with the *worst-case* assumption when compared to the Freundlich isotherm of Schaefer et al. (2019) since K_{awi} for the Langmuir isotherm is constant at sufficiently low aqueous concentrations. However, investigating the input files of the modified version it appears as though it is not possible to model both non-linear solid adsorption and non-linear AWI adsorption, unless they coincidentally are parameterised the same. This is because a parameter (nu) is used for both the solid phase adsorption isotherm and the AWI adsorption isotherm. The reason for this is not sure (maybe it was overlooked, or I am misinterpreting) but it does limit the capabilities to only linear isotherms. However, this is not all bad since the full capabilities of Hydrus are still available.

The modified version has been tested to see if the implementation works as expected, and the results indicate that implementation was done correctly. Briefly put, Simunek et al. set up a set of scenarios in which only one retention mechanism was “turned on” per scenario (i.e. each scenario had partitioning to either gas, solid, or AWI), and parameterized it such that the results should be identical, which they were. This modified version of Hydrus could be used to develop more complex scenarios, including transient flow conditions.